6-9-2016

Effects of the Fiber Distribution and Number of Nearby Fibers on the Thermal Conductivity for Aligned CNT-Silicon Oil Composites

Diana Grandio
Santa Clara University

SANTA CLARA UNIVERSITY
Department of Mechanical Engineering

June 9th, 2016

I HEREBY RECOMMEND THAT THE THESIS PREPARED UNDER MY SUPERVISION BY

Diana Grandio

ENTITLED

Effects of the fiber distribution and number of nearby fibers on the thermal conductivity for aligned CNT-silicon oil composites.

BE ACCEPTED IN PARTIAL FULFILLMENT OF THE REQUIREMENTS FOR THE DEGREE

OF

MASTER OF SCIENCE IN MECHANICAL ENGINEERING

DRAZEN FABRIS, THESIS ADVISOR

ON SHUN PAK, THESIS READER

DRAZEN FABRIS, CHAIRMAN OF DEPARTMENT

EFFECTS OF THE FIBER DISTRIBUTION AND NUMBER OF NEARBY FIBERS ON THE THERMAL CONDUCTIVITY FOR ALIGNED CNT-SILICON OIL COMPOSITES.

BY

DIANA GRANDIO

MASTER OF SCIENCE THESIS

SUBMITTED IN PARTIAL FULFILLMENT OF THE REQUIREMENTS
FOR THE DEGREE OF MASTER OF SCIENCE
IN MECHANICAL ENGINEERING IN THE SCHOOL OF ENGINEERING
SANTA CLARA UNIVERSITY, 2016

SANTA CLARA, CALIFORNIA, USA

Abstract

Carbon Nanotubes (CNT) are seen as promising materials for thermal transport applications. The high thermal conductivity and structural flexibility of the CNT present them as very attractive components to be used as particle fillers in thermal interface materials. It is important to understand the effective thermal conductivity for CNT-matrix composites at high CNT volume fraction.

In prior work, an effective medium approach (EMA) has been developed to evaluate composite physical properties such as thermal conductivity, dielectric function or elastic modulus (C-W Nan, Prog. Mat. Sci. V 37, 1993). This model combined with the Kapitza interface resistance can predict the effective thermal conductivity of randomly dispersed long fibers for a very low volume fraction ($f < 0.01$). The interfacial contact resistance is a combination of poor mechanical or chemical adherence at the interface and thermal expansion mismatch between the particle and the matrix. Many studies have demonstrated that the Kapitza resistance has an important impact on the effective thermal conductivity of composites.

The present study compares finite-element (FEA) computations and the EMA model for CNT-matrix compositions with low to moderate volume fractions, 0.001 to 0.02. The value of the Kapitza radius used for the estimation of the interface resistance between the CNT and the matrix is obtained from values calculated in literature. In the simulation, the thermal conductivity of the particle filler is considered orthotropic due to the added Kapitza resistance. A comparison is calculated according to the EMA model. To determine the particle to particle interaction the different geometric configurations are evaluated by using Voronoi cells. This is a tool for characterization of composite materials, identifying the closest particles or near neighbors.

The FEA results obtained show that the EMA model underestimates the effective thermal conductivity of the composite when the particles are very close to each other. The present work proposes a general correction function for the dependence on the particle to particle interaction based on the near neighbor distances and the number of near neighbors. This correction function for particle to particle interaction is tested for various configurations and reduces the EMA over prediction to within several percent (< 5%) in most cases.

Contents

List of figures.

List of tables.

NOMENCLATURE

AN	average number of near neighbors
d	diameter of carbon nanotube
EMA	Effective Medium Approach
f	volume fraction
FEA	Finite Element Analysis
k	thermal conductivity (W/mK)
$k_{CNT\text{-}matrix}$	thermal conductivity in the fiber-matrix region
k_{corr}	correction factor (W/mK)
k_{ii}^{c}	thermal conductivity of the fiber in the X_i symmetric axis
k_{ii}	thermal conductivity of the composite in the X_i symmetric axis
k_m	thermal conductivity of the matrix
k_p	thermal conductivity embedded particle
k_T	total thermal conductivity
L	fiber length
L_{ii}	geometrical factor
L_T	matrix length
MNND	mean near neighbor distance.
NND	near neighbor distance
p	aspect ratio
R_{tc}	thermal resistance TIM
R_{ci}	contact thermal resistance
R_b	thermal resistance at the interface fiber-matrix
VF	volume fraction (%)

Chapter 1. Introduction

1.1 Thermal management of electronics cooling.

The rapid advances in miniaturization of electronic components are accompanied by an increase in transistor density and a rise in the clock frequency of integrated electronic circuits. Those factors contribute to a notable increase in the heat generation in the electronic chips. Electronic chips are normally cooled by forced air convection. The next generation of electronics will demand more compact and efficient cooling techniques to operate in the required temperature ranges.
Nowadays, thermal management of electronics cooling is one of the main concerns of computers companies and users [1]. The new technologies in the electronics industry are limited by the problem of thermal cooling. More than 50% of the

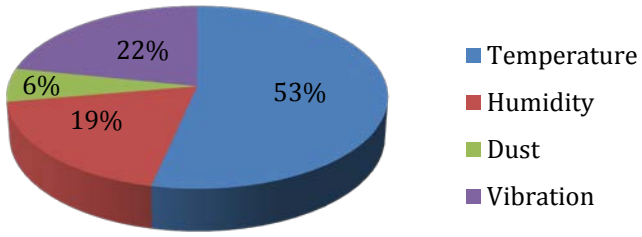

Figure 1. Major causes for electronics failure. High temperatures are most common cause of failure [61].

failures of electronics are related to poor thermal management. The failure rates increase exponentially with the temperature of the junction. For every 10^0C temperature increase in the chip junction temperature the failure rate doubles. This affects directly to the reliability of the electronic system [2].
Thermal cooling of electronic components basically consists of the heat removal from the heat source to a heat spreader. In *Figure 2* are shown two typical schemas for chip thermal cooling. The first one (a) is a typical system used in laptop applications. The heat is transfer from the die to the heat sink through a thermal interface material. In the second case (b) the heating pathway is very similar. Effective heat removal depends on the conduction from the chip to the heat dissipation device.

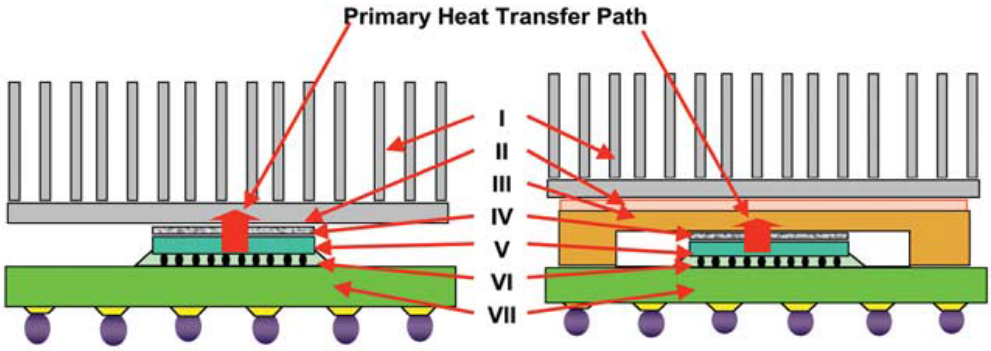

Figure 2. I-Heat Sink, II-TIM, III-HIS, IV-TIM, V-die, VI-Underfill, VII-Package substrate
(a) Thermal management system typically used in laptop applications. (b) Thermal management system typically used in desktop and server applications. [5]. **IEEE copyright© 2006 IEEE**

One of the main challenges in thermal management is the thermal resistance between contacting components. Very often these resistances limited the performance of optimized thermal packages. The contact resistance between components is the limiting factor. When two surfaces are contacting, the non-perfect flatness of the different surfaces is going to limit the contact between the two surfaces. The flow heat across the interface involves heat conduction across the contacting areas and conduction through the fluid that it is occupying the free areas. This fluid is normally air, and it has a very low conductivity. It is estimated that just 1-2% of the area of slightly loaded interfaces is contacting with no air in between.
On the top of thermal resistance due to the surface roughness, the chip surface (Si die) due to thermal expansion is typically warped, Figure 3. The deformation of the Si die depends on various factors as geometry of the substrate, mismatch of the thermal expansion coefficient between the substrate and the die and the temperature. Due to this phenomenon the area of contact between the chip and the heat sink will reduce compared to a flat surface, meaning an increase of the thermal resistance between surfaces.
The contribution of the thermal resistances between contacting surfaces for heat removal often accounts for more than 30% of the overall thermal resistance [3]. If the resistance through the interface is high enough that the heat cannot be removed from the electronic component, this can fail due to thermal runaway.

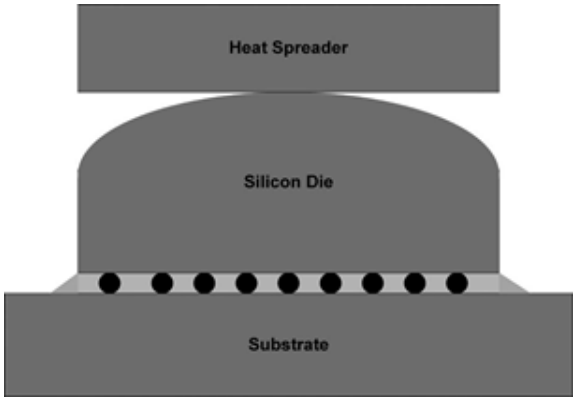

Figure 3 . Representation (not a scale) of a warped die [5]. **IEEE copyright © 2006 IEEE**

Thermal interface materials are thermal connections placed between contacting surfaces in electronic packages. They play a key role improving the overall heat transport and reduce the thermal resistance. Thermal interface materials facilitate a pathway for heat to be transferred from the chip to the heat sink. Reducing the contact resistance will enable to design simpler and smaller heat cooling devices for more compact electronics devices.
Improvement of the thermal interface materials shall reduce costs associated with heat sinks and cooling fans. It has been speculated that an improvement of 30% of the performance of the thermal interface materials can lead to a 17% improvement of the overall heat removal in electronic packages and 24% cost reduction in the cooling system. This fact generates a cost reduction that can exceed tens of millions of dollars per year [3].

1.2 Thermal interface materials

Thermal interface materials are high conductive materials placed in between components to enhance the heat transfer between them. They are considered as composite materials and consist of high conductivity particles embedded in a soft matrix able to create a seamless contact between surfaces by filling the surface voids.
The total resistance opposed to transferring heat between two solid contact surfaces is characterized by a discontinuity in the temperature profile in the direction of the heat transfer, Figure 4. This temperature change is attributed to the thermal contact resistance and it is defined as the ratio of the temperature difference between the two contacting surfaces (ΔT) and the heat flux normal to the interface (Q) [4].

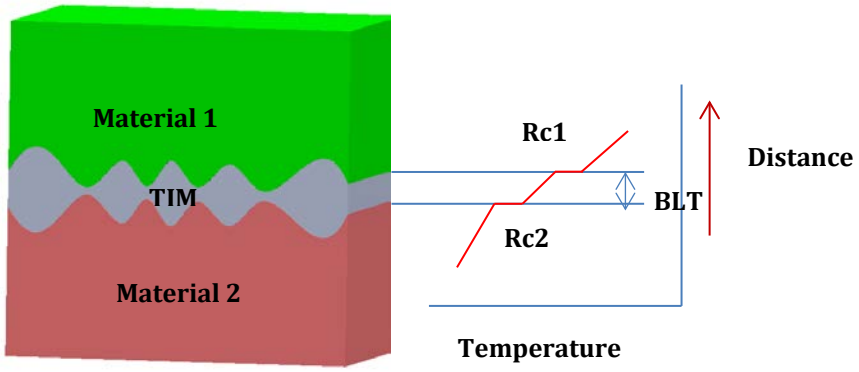

Figure 4. Schematic of a Thermal Interface Materials [62]

$$R_{tc} = \frac{\Delta T}{Q} \qquad (1)$$

The total thermal resistance can be seen as a sum of three resistances in series, the thermal resistance of both contacting surfaces (Rc_1 and Rc_2) and the thermal resistance of the bulk material (BLT/k_{TIM}) [5]:

$$R_{tc} = \frac{BLT}{k_{TIM}} + R_{c1} + R_{c2} \quad (2)$$

The thermal resistance of the thermal interface material is equal to the ratio of the bond line thickness (BLT) and the bulk thermal conductivity on the material.
From equation 2 we can deduce that TIM performance is dependent on three main factors [5]:
1) Thermal conductivity of the thermal interface material (k_{TIM})
2) Bond line thickness of the thermal interface material (BLT)
3) Thermal boundary resistance between the thermal interface material and the two solid surfaces (Rc_1 and Rc_2).
To get a good understanding of the variables affecting the overall thermal resistance between contacting surfaces the factors named above will be briefly explained, emphasizing more on the thermal conductivity of the bulk material as it is the main focus of this work.

BLT: Bond line thickness

The bond line thickness of thermal interface materials depends on the yield stress and the applied pressure [6]. Polymeric thermal interface materials are the most common used in electronics cooling [7], [8]. Thermal interface materials are considered as semisolid and semiliquid materials.
The bond line thickness of a thermal interface material changes once pressure is applied and it is different for different pressures. It reaches a constant value after some time (steady state). The bond line thickness also increases with the particle volume fraction. Some studies have shown that after a certain particle volume fraction the thermal resistance of the thermal interface material starts to increase. It is believed that high volume fraction can increase the contact resistance between the thermal interface materials and the adjoining surfaces [6]. Prasher [9] showed that there is an optimum particle volume fraction for the minimization of the thermal resistance for a given pressure and a filler shape. He developed a model called the scaling-bulk model (S-B) where the bond line thickness is calculated as [9]:

$$BLT = \frac{2}{3} r \left\lfloor c \left(\frac{d}{BLT}\right)^{4.3} + 1 \right\rfloor \left(\frac{\tau_y}{P}\right)^m \quad , \quad (3)$$

where m and c are empirical constants, r is the radius of the particle, τ_y is the yield stress of the polymer and P is the pressure applied. Equation 3 can be simplified as:

$$\text{For low } \left(\frac{\tau_y}{P}\right) \text{ it reduces to BLT}=c \left(\frac{\tau_y}{P}\right)^m \quad (4)$$

$$\text{For high } \left(\frac{\tau_y}{P}\right) \text{ it reduces to BLT} = \frac{2}{3} r \left(\frac{\tau_y}{P}\right) \quad (5)$$

This model is based on the assumption that polymeric thermal interface materials behave as Herschel-Bulkely fluid. Other authors tried to model the bond line thickness polymeric thermal interface materials considering they behave as Newtonian fluids, but this assumption led to the conclusion that the optimum bond line thickness shall be zero [10].
The bond line thicknesses combined with the thermal conductivity model are used for modeling the thermal resistance of the bulk thermal interface material.

Thermal contact resistance

Thermal contact resistances in micro composites are not as predominant as the thermal resistance of the bulk material [11].This conclusion was obtained in Intel after some studies on various internal interface materials. Although, it plays an important role in determining the heat flow transferred from the heat source to the thermal interface material; however, in nanostructure/substrate contacts thermal contact resistance is a very important issue. Those contacts are not perfect welded contacts due to weak van de Waals forces. Some studies have shown that the thermal contact resistance of nanocomposites is characterized by the phonon equilibrium intensity and the transitivity of phonons across the interface [12]. Thermal contact resistance can be affected by temperature and size of the embedded particles. The thermal contact resistance for micro composites is the same as the matrix for nominal values fractions, but for nanocomposites, the thermal contact resistance is modified due to the phonon scattering especially at low temperatures.
Prasher [13] developed and acoustic mismatch model for thermal contact resistance where the conductance at the interface is proportional to the square of the adhesion energy. Thermal interface materials adhere to the surface substrate through van der Waals forces. Van der Waals forces are weak adhesive forces. Those weak forces have low energy adhesion, a fact that difficulty the heat transfer across the surface creating high contact resistances at the interface nanostructure/substrate. Kaur [14] corroborate Prasher's model and he showed that bridging carbon nanotubes with covalent linkers to the substrate increase both thermal transport and mechanical adhesion.

Thermal conductivity

There are many theoretical and empirical relations to predict the thermal conductivity of solid filled composites. Progelhof *et al.* [16] presented a review of the methods available to predict the thermal conductivity of composites and they conclude that there are not accurate techniques or correlation valid for all types of composites. Many theoretical models do not include the interfacial resistance on the particle/matrix surface. The interfacial contact resistance is associated with the combination of poor mechanical or chemical adherence at the interface or a thermal expansion mismatch between the particle and the matrix. The interfacial resistance

in a composite between the particle and the matrix is called Kapitza resistance [19], name after Kapitza's discovery of temperature discontinuity at the metal-liquid interface [20]. Many studies have demonstrated that the Kapitza resistance has an important impact on the effective thermal conductivity in composites [21].

As mentioned before, thermal interface materials consist of a very low conductivity base material, grease or polymer, fill in with high conductive particles. The effective thermal conductivity of the composite is dependent of the thermal conductivity of the fillers, the thermal conductivity of the matrix, the fillers volume fraction and the interface resistance between fillers and matrix. Due to this large contrast in conductivities between the fillers and the matrix, Depvura *et al.* [15] proposed a model for the effective thermal conductivity calculation called percolation model. This is a geometrical model that proposes that at certain volume fraction (percolation threshold) it is created a continuous path for the heat to be transferred because the conducting particles start to touch each other. The percolation model is valid when $k_P/k_m \to \infty$ [5]. This is possible for electrical conductivity, as there are materials that are perfect insulators, but for thermal conductivity is not possible, there are no materials that present zero conductivity. Another consideration is that spherical and cylindrical particles due to the curvature of their surface will present constriction/spreading of heat flow in the particle and matrix interface. This effect is not considered in the percolation model.

By applying the percolation model, composites fill in with carbon nanotubes with a concentration above the percolation threshold predict an increase in the thermal conductivity of 50 fold compared to the conductivity of a composite with 1% volume of carbon nanotubes [17]. Direct experimentation showed that this prediction was far lower. This fact suggested that the resistance at the interface is the responsible of the low thermal conductivity. M.B. Bryninh *et al.* [18] reported the thermal conductivity of SWNT composites in N-N- Dimethylformamide (DMF) and surfactant

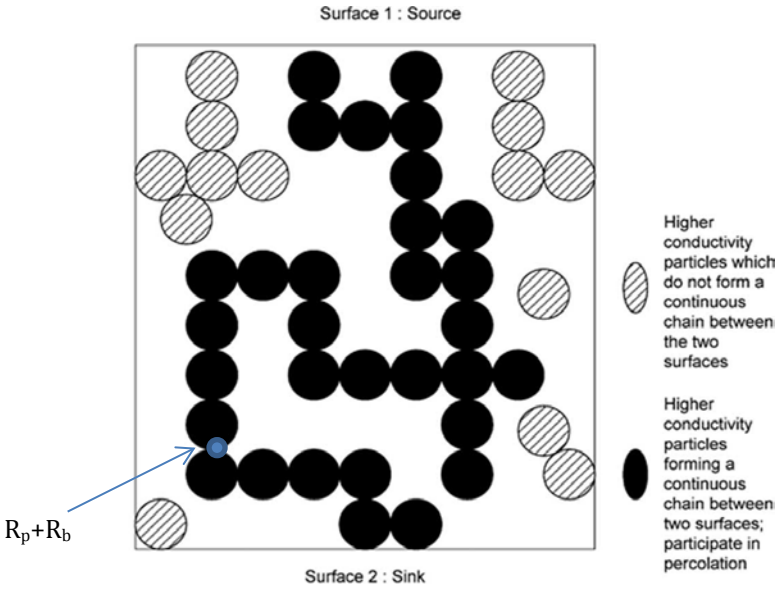

Figure 5. Schematic of a TIM with spherical fillers showing one percolation path [5]**. IEEE copyright © 2006 IEEE**

R_b= Interfacial boundary resistance particle-matrix, R_p=Interfacial boundary resistance particle-particle.

stabilized suspensions. They observed less enhancement of the thermal conductivity of the composites with surfactant stabilized. It was attributed to the difference in the interfacial resistance between the particles and the matrix. The surfactant coats the SWNTs and it reduces the heat transfer.
There are two theoretical approaches to predict the Kapitza resistance. One of them is called the acoustic mismatch model (AMM). In the AMM the propagation of waves is deterministic, and the transmission and reflection coefficients for phonons are given by classical wave propagation formulas [22]. The other approach is called the diffuse mismatch model (DMM). This model is considered stochastic. The DMM model considers that the phonons at the interface are scattered to the adjacent material with a probability proportional to the phonon density of states in the receiving material [23]. With the existing models is difficult to estimate a value of thermal resistance at the different composites, only experimental analysis to estimate the Kapitza resistance can be done.
Nan [21] [24] proposed a theoretical model to estimate the effective thermal conductivity including the effect of the interfacial resistance. This model was called effective medium approach (EMA) and it considers the multi-scattering theory on nanocomposites. The model was developed to predict the thermal conductivity of ellipsoidal particles, but the results can be applied to axially aligned fibers, laminated flat plates and spheres by using the corresponding geometry factors.
Some theoretical analysis has been performed to predict the effective thermal conductivity of composites following the EMA approach introduced by Nan. Hasselman and Johnson [25] carried out the first theoretical analysis. They consider simply spherical particles embedded in a matrix and derived a Maxwell-Garnett type effective medium approximation (MG-EMA) to calculate the effective thermal conductivity considering the interface thermal resistance and the particle size for spherical particles. For nonspherical particles, Hatta and Taya [26] and Benveniste and Miloh [27] proposed several analytical models to predict the effective conductivity of composites containing aligned or randomly oriented short fibers.
To summarize the effective thermal conductivity of a composite is not a just function of the volume fraction of the high conductive particles embedded in the matrix, the Kapitza resistance plays an important role and it should not be neglected.
The work of this thesis is based on the effective medium approach (EMA) proposed by Nan [24]. A more detailed discussion of this theory will be explained in chapter 2.

1.3 Carbon nanotubes as highly conductive materials.

Carbon nanotubes were discovered by Sumio Iijima in 1991 [28]. The configuration of a carbon nanotube is equivalent to a single (single wall) or multiple (multiwall) two-dimensional graphene(s) sheets rolled into a tube. They have excellent properties. Carbon nanotubes are a very strong and flexible material because of the C-C covalent bonding. They have a Young's modulus of 1 TPa [29] versus for example aluminum that has 70GPa. The strength to weight ratio is 500 times higher

than aluminum. Carbon nanotubes have an excellent electrical conductivity, presenting a current carrying capacity of 10^7-10^9 A/cm^2 [30]. They can behave as metallic or semiconducting depending on the chirality. Carbon nanotubes also present excellent thermal properties. They have a huge thermal conductivity. The conductivity of 3000 W/mK [31] has been demonstrated for a multiwall carbon nanotube. Carbon nanotubes also allow other chemical groups to be attached to the tip or sidewall (functionalization) [31].

For all those reasons carbon nanotubes seem as a promising material for many electrical, structural and thermal applications. The huge thermal conductivity and structural flexibility convert the carbon nanotubes as a very attractive material for many types of research to use it as thermal interface materials.

The use of carbon nanotubes as thermal interfaces materials is still at an early stage. There are still some challenges that need to be addressed. Some of those challenges are related to the fabrication processes. It is difficult to obtain a homogeneous dispersion of carbon nanotubes in host materials. Also, their chirality is not easy to control, affecting the controllability of their electrical conductivity. Being not able to control the electrical conductivity of a material used in electronics can be a concern for some applications.

Despite those challenges, carbon nanotubes seem a promising material to be used as filler in thermal interface materials. Many efforts have been done in the last years studying the effective thermal resistance of carbon nanotubes based thermal interface materials.

As explained above, thermal interface materials are comprised of a base material (grease or polymer) with thermally conductive fillers like metal and ceramic powders and carbon-based materials. Normally, the thermal conductivity of the base materials ranges between 0.1-0.3 W/mK [32]. In Table 1 are presented the thermal conductivities of the most common materials used as thermal fillers in thermal interface materials and also some composites. As it can be easily seen the thermal conductivity of carbon nanotubes is more than 100 times that most of the materials used.

The carbon nanotubes used as fillers for thermal interface materials present a high aspect ratio. Those long and thin tubes create a higher area for the heat to be transferred. Nielsen *et al*. [33] demonstrated that using rods with a high aspect ratio as fillers present a thermal conductivity of approximately 40% higher compared to spherical fillers for the same concentration. Composites with carbon nanotubes fillers show an enhancement in the thermal conductivity at low concentrations [32]. 0.1% wt of carbon nanotubes incorporate in grease or polymeric matrix can theoretically enhance the thermal conductivity six-fold. Those are promising values but experimental results show that with current fabrication techniques is still not possible to obtain those promising values for the thermal conductivity of composites [34] [35] [36] [37]. The thermal conductivity of traditional particle-laden polymeric thermal interface materials is within the range 1-10 W/mK [38]. In comparison with other nanostructured materials, carbon nanotubes provide the greater enhancement of thermal conductivity. Xu and Fisher studied the thermal resistance of multiwall carbon nanotubes synthesized directly in silicon wafers in a high-vacuum environment with radiation shielding [40]. Choi *et al.* measured the

effective thermal conductivity of nanotube-in-oil suspensions.The experimental results obtained were greater than theoretical predictions and they presented a non-linear relation

Table 1. Thermal conductivity of common fillers and composites **[39]**.

Material	**Thermal Conductivity (W/mK)**	**Material**	**Thermal Conductivity (W/mK)**
Aluminum	234	Boron Nitride	110
Gold	315	Rubber+Al2O3	0.6
Lead	30	Epoxy +Carbon fiber	300
Diamond	1300-2400	Aluminum oxide	18
Carbon fiber	260	Aluminum nitride	200-320
Silicon Nitride	30	Commercially electrically non-conductive plastics	1-10

between thermal conductivity and carbon nanotubes loading [41]. Biercuk *et al.* showed that epoxy loaded with 1 wt% of SWNT presented an increase of 70% of the thermal conductivity at 40K, increasing to 125% at room temperature [42]. Xuejiao Hu *et al.* showed that small quantities of CNT inclusions can improve the thermal conductivity. Based on closed-form model to account for the interaction between CNT and metal particles, it was obtained an enhancement of the thermal conductivity with an inclusion of 1.4 wt% CNT in a composite of 40 wt% nickel particles, and also for 2.2 wt% CNT in a 30% nickel particles composites [43]. Fabris *et al.* compared the thermal conductivity of commercial TIM with CNT inclusions and CNT-silicon oil composites. They observed an improved performance in the CNT-silicon oil composites at increased load of CNT at high pressures [44]. The anomalous enhancement of the thermal conductivity is theoretically intriguing. Some models have been proposed to estimate the effective thermal conductivity of the CNT-based thermal interface materials.

Previous research on CNT composites has been done at Santa Clara University. A steady state thermal resistance measurement based on the ASTM D5470-06 standard was design to measure the thermal resistance of CNT-silicon oil composites. The thermal resistance was measured at constant heat rate and different contact pressure 0.0069-0.758 MPa. The CNT concentration in the CNT-silicon oil matrix was 0.0099-0.99%. At low concentrations, approximately 0.0099% the measured effective thermal conductivity increased by 22%, while at high concentrations 0.99% the thermal conductivity decreased. Those results can be explained by an increase on the interface resistance at high concentrations. This work showed some factors as interface resistance and the disposition of the carbon nanotubes inside the matrix may have some effect on the thermal resistance. The present work tries to get a better understanding of the thermal behavior of CNT polymeric composites and how they can be improve to achieve better performance.

Chapter 2. CNT-polymer composites

2.1 Model for predicting thermal conductivity of CNT-Polymer composites.

The model proposed by Nan [21] [24] can predict the effective thermal conductivity of randomly dispersed long fibers for a very low volume fraction (f<0.01) [45]. It considers the effect of the interfacial resistance between the conductive particles and the fillers on the effective thermal conductivity. Some other theoretical models have been used to predict the effective thermal conductivity of composites fill in with carbon nanotubes, as the percolation model proposed by Depvura *et al*. [15]. As explained in Chapter 1, most of those theoretical models do not include the interfacial resistance that has an important effect on the effective thermal conductivity. The objective of the present work is to compare the results provided by the EMA model with FEA analysis of CNT-polymer composites. The effective thermal conductivity provided by the EMA model shall be similar to the thermal effective conductivity calculated by FEA thermal analysis if the model is accurate. First, the EMA model is explained to get a good understanding of all the assumptions taken in the model.

Effective medium theory (EMA) with interface thermal resistance.

The effective medium approach is a method to evaluate the variation with space of physical properties as thermal conductivity, dielectric function or elastic modulus. This variation can be linear or nonlinear. This work will focus on the linear variation of the thermal conductivity with respect to space in a homogeneous medium (composite). Nan [21] combined the effective medium approach with the Kapitza thermal contact resistance and developed a model that predicts the effective thermal conductivity of fibers particles based composites.

General modelling.

In most heterogeneous materials, their physical properties cannot be predicted in terms of so-called "mixtures rules''. This method predicts a physical property of a heterogeneous material based just on the volume fraction of the different components forming the material. These rules cannot be applied to predict the effective thermal conductivity of composites [24]. There are several approaches to predict the microstructure-property relationships, as homogenization method, variation at principles, first-principle approach, statistical analysis and effective medium theories. The effective medium approach (EMA) is one of the most used in predicting the microstructure properties. Based on the multiple scattering theory it can be developed a general formulation of the EMA (effective medium approach) for the effective thermal conductivity of arbitrary particulate composites with

interfacial thermal resistance [21]. It is assumed that the thermal conductivity has a linear variation from point to point and it can be expressed as

$$k(r)= k^0+k'(r) \quad (6)$$

where k^0 is the constant part of the homogeneous medium and $k'(r)$ is the fluctuating part.

The thermal conductivity of the homogeneous part is assumed to be equal as the thermal conductivity of the matrix. Applying the Green function G [46] and the transition matrix T for the entire composite medium, the effective thermal conductivity can be expressed as

$$k_{effective}=k^0+ \langle T\rangle(I+\langle GT\rangle)^{-1} \quad (7)$$

where I is the unit tensor and $\langle\ \rangle$ is the spatial averaging.

The matrix T is defined as

$$T=\sum_n T_n + \sum_{n,m\neq n} T_n\, GT_m + \cdots, \quad (8)$$

The first term is the sum of the matrices of n particles. The successive terms represent the interaction between particles. This model assumes that the particles

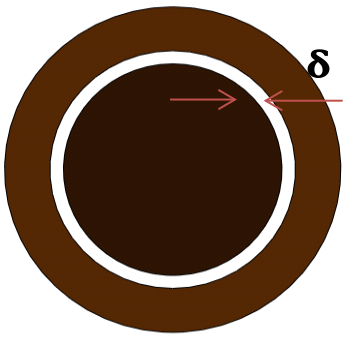

***Figure 6**. Interface resistance between the particle and the matrix.*

are dispersed in the matrix, and for that reason, they do not interact with each other. With this assumption the term related to the interaction between particles can be neglected and Equation 8 can be rewritten as:

$$T \cong \sum_n T_n = \sum_n k'_n(I - Gk'_n)^{-1} \quad (9)$$

This assumption is valid for a very small volume fraction of filler particles, f<0.01.

The interface resistance is going to be determined by the interface layer. The interface layer is generated due to a poor mechanical or chemical adherence at the interface of the particle and the matrix, and it is denoted as δ. It is assumed that the thickness of the surrounding interface layer is minimum ($\delta\rightarrow 0$). The conductivity of the interfacial layer is composed of a poorly conductive region and it is assumed to have very small thermal conductivity ($k_s\rightarrow 0$). The thermal conductivity of the host material (matrix) is also very small. It can be assumed that the thermal conductivity

of the interface particle/matrix is the same as the thermal conductivity of the matrix (k_s=k_m).
The CNT- based composites are filled with CNT of very high aspect ratio. Those long fibers will present orthotropic thermal conductivity. The thermal conductivities k_{ii}^c $(i = 1,2,3)$ along the X_i' symmetric axis of a fiber embedded in a host material can be expressed as

$$k_{ii}^c = k_p/(1 + \frac{\gamma L_{ii} k_p}{k_m}) \tag{10}$$

k_p and k_m are the thermal conductivity of the embedded particle and the matrix respectively. L_{ii} is a geometrical factor that depends on the particle shape. p is the aspect ratio of the fiber and it is defined as the ratio between the length and the diameter p=L/d. The factor γ is a function of the Kapitza resistance and the aspect ratio.

$$\gamma = \begin{cases} \left(2 + \frac{1}{p}\right)\alpha, & for\ p \geq 1 \\ (1 + 2p)\alpha & for\ p \leq 1 \end{cases} \tag{11}$$

$$\propto = \begin{cases} \frac{a_k}{d} & for\ p \geq 1 \\ \frac{a_k}{L} & for\ p \leq 1 \end{cases} \tag{12}$$

$$L_{11} = L_{22} = \begin{cases} \frac{p^2}{2(p^2-1)} - \frac{p}{2(p^2-1)^{3/2}} \cosh^{-1} p & for\ p > 1, \\ \frac{p^2}{2(p^2-1)} + \frac{p}{2(1-p^2)^{3/2}} \cosh^{-1} p & for\ p < 1, \end{cases} \tag{13}$$

$$L_{33}=1-2L_{11} \tag{14}$$

The Kapitza resistance is defined as the ratio between the temperature drop and the heat flux at the interface. It is calculated based on the principles of conducting heat

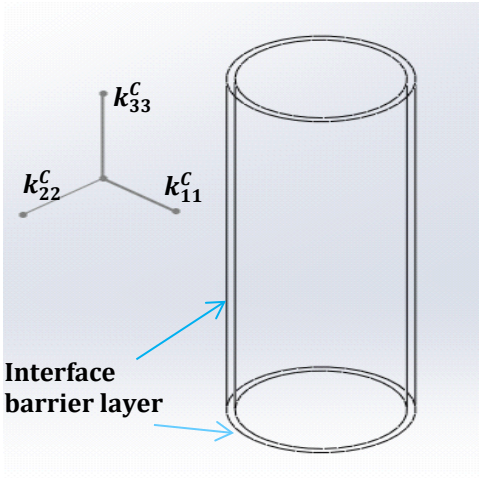

Figure 7. Illustration of a the transverse and longitudinal thermal conductivities of a composite unit cell of a nanotube coated with a very thin interface layer [45]

transfer between two solids. The resistance at the interface is associated with a minimum interface layer thickness with a very poor thermal conductivity. The Kapitza radius introduces the concept of interface thermal resistance and it is equal to zero (a_k =0) in a perfect interface. It is defined as the product of the thermal resistance at the interface and the thermal conductivity of the matrix.

$$a_k = R_{bd} k_{m,} \quad with\ R_{bd} = \lim_{\substack{\delta \to 0 \\ k_s \to 0}} \left(\frac{\delta}{k_s}\right) \tag{15}$$

There are not theoretical models that can predict the Kapitza resistance accurately. Those values differ from composite to composite. Experimentation is required to get a good approximation of the Kapitza resistance.
Based on Equations 6 -15 a general expression for the effective thermal conductivity (EMA) in the directions perpendicular to the heat flux (k_{11}^* and k_{22}^*) and in the direction of the heat flux (k_{33}^*) of a composite can be written as:

$$k_{11}^* = k_{22}^* = k_m \frac{2+f[\beta_{11}(1-L_{11})(1+\langle\cos^2\theta\rangle)+\beta_{33}(1-L_{33})(1-\langle\cos^2\theta\rangle)]}{2-f[\beta_{11}L_{11}(1+\langle\cos^2\theta\rangle)+\beta_{33}L_{33}(1-\langle\cos^2\theta\rangle)]} \tag{16}$$

$$k_{33}^* = k_m \frac{1+f[\beta_{11}(1-L_{11})(1-\langle cos^2\,\theta\rangle)+\beta_{33}(1-L_{33})\langle cos^2\,\theta\rangle]}{1-f[\beta_{11}L_{11}(1-\langle cos^2\,\theta\rangle)+\beta_{33}L_{33}\langle cos^2\,\theta\rangle} \tag{17}$$

$$\beta_{ii} = \frac{k_{ii}^c - k_m}{k_m + L_{ii}(k_{ii}^c - k_m)} \tag{18}$$

$$\langle\cos^2\theta\rangle = \frac{\int \rho(\theta)\cos^2\theta\sin\theta\, d\theta}{\int \rho(\theta)\sin\theta\, d\theta} \tag{19}$$

where θ is the angle between the materials axis X_3 and the local particle symmetric axis X'_3, $\rho(\theta)$ is a distribution function describing the particle orientation and f is the volume fraction of the particles.
The EMA model explained above is a general form and it can be applied to different particles shapes. In the following sections, it is explained two cases of interest for the present work.

Axially aligned fibers.

The ideal case is that the fibers embedded in the matrix are aligned and parallel to the heat flux direction.
For long fibers is assumed that $p \to \infty$. For a high p ratio, over 100, the geometrical factors are constant and equal to L_{11}= L_{22}=0.5 and L_{33}=0 [21]. If the fibers are oriented parallel to the X_3 axis then $\langle\cos^2\theta\rangle$=1 and Equation 10 can be reduced to

$$k_{11}^c = k_{22}^c = k_p/(1 + \frac{\propto k_p}{k_m}) \tag{20}$$

$$k_{33}^{c} = k_p \tag{21}$$

Equations 20-21 estimate the thermal conductivity of one single fiber considering the thermal resistance at the interface in the transversal and longitudinal direction of the fiber. It can be appreciated that the thermal resistance at the interface is just affecting the heat transfer in the transversal direction. In the longitudinal direction, the thermal conductivity is the same as the thermal conductivity of the fiber not surrounded by a host material. The EMA approach considers that for aligned continuous fibers the interface resistance is not affecting the thermal conductivity in the longitudinal direction in the fiber.

The same conclusion is obtained for the effective thermal conductivity of the composite. Equations 22-23 estimate the thermal conductivity of the composite in the perpendicular and parallel direction of the heat flux. The model assumes that for the direction of the heat flux the thermal conductivity of the composite is just depending on the volume fraction of the fibers.

$$k_{11}^{*} = k_{22}^{*} = k_m \frac{k_p(1+\propto)+k_m+f[k_p(1-\propto)-k_m]}{k_p(1+\propto)+k_m-f(k_p(1-\propto)-k_m]} \tag{22}$$

$$k_{33}^{*} = (1-f)k_m + fk_p \tag{23}$$

The present work shows that the Kapitza resistance cannot be neglected in the longitudinal direction, even for axially aligned fibers. Not considering the interfacial resistance will lead to a notable overestimation of the effective thermal conductivity of the composite.

Long fibers randomly dispersed in a matrix.

The effective medium approach can also be applied to fibers randomly dispersed in a matrix. For very long fibers the aspect ratio is assumed $p \rightarrow \infty$, and the geometrical factors L_{11}=L_{22}=0.5 and L_{33}=0. For fibers randomly distributed the $\langle cos^2\,\theta \rangle$=0 [45] [47].

Applying the assumptions described above the thermal conductivity of one single fiber can be expressed as:

$$k_{11}^{C} = k_{22}^{C} = \frac{k_p}{1+2\frac{a_k}{d}\frac{k_p}{k_{matrix}}} \tag{24}$$

$$k_{33}^{C} = \frac{k_p}{1+2\frac{a_k}{L}\frac{k_p}{k_{matrix}}} \tag{25}$$

where k_{11},k_{22} represents the thermal conductivity in the transversal direction and k_{33} the thermal conductivity in the longitudinal direction. This case assumes that the interface thermal resistance is affecting both directions. The factor $\propto$ from Equation 12 is defined as follows

$$\propto = \begin{cases} \frac{a_k}{d} & \text{for the tranversal direction } k_{11}, k_{22} \\ \frac{a_k}{L} & \text{for the longitudinal direction } k_{33} \end{cases} \quad (26)$$

Applying the assumptions above to Equations 16- 19 the effective thermal conductivity of composite fill in with randomly dispersed long fibers can be expressed as:

$$k_{effective} = \frac{3+f(\beta_{11}+\beta_{33})}{3-f(\beta_{11})} \quad (27)$$

$$\beta_{11} = \frac{2(k_{11}^C - k_{matrix})}{k_{11}^C + k_{matrix}} \quad (28)$$

$$\beta_{33} = \frac{k_{33}^C}{k_{matrix}} - 1 \quad (29)$$

The equations obtained for this special case assume that the Kapitza resistance is affecting the thermal conductivity in all the directions.

2.2 Characterization of composite microstructures by Voronoi cells.

The physical properties of a composite are dependent on the size, shape and spatial distribution within the host material. Brockenbrough *et al.* showed that for a composite filled in with long fibers both the fiber shape and the distribution were affecting the tensile and shear deformations, and this effect was more notorious for high fiber volume fractions [48]. Chistman *et al.* concluded that clustering has a significant effect in reducing strain hardening on metal-ceramic composites [49]. All

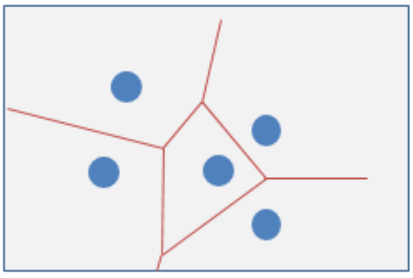

Figure 8.Voronoi Diagram

those studies manifested the necessity for the account of the spatial distribution of the filler particles in a composite [50]. Gosh *et al.* presented a microstructure based Voronoi Cell Finite Element Model (VCFEM) for modeling heterogeneous materials with arbitrary dispersions [51] [52] [53] [54]. This model combines concepts of finite element methods and essential micromechanics requirements to obtain an

effective representative element material (REM). The VCFEM method uses the Voronoi cells resulting from Dirichlet tessellation of planar heterogeneous microstructures.
In heterogeneous composites, the identification of clusters and the estimation of the distances between particles is a very important factor to predict the inter-particle interactions. Voronoi cells are a tool used for the characterization of heterogeneous materials. They are a very useful tool to estimate the closest particles or near neighbors.
The mathematical definition of a Voronoi diagram is as follows:

Given at set S of n points $p_1, p_2, \ldots, p_n$ in a plane, the Voronoi diagram divides the plane into n Voronoi regions. Voronoi diagrams present the following properties [55]:

1. Each Voronoi region present exactly one point p_i.
2. If a point $q \notin S$ lies in the same region of p_i, then the Euclidian distance from pi to q will be shorter than the Euclidian distance from p_j to q, where p_j is any other point in S.
   Euclidean_Distance (q,p_i)<Euclidian_Distance (q,p_j) for each $p_i \in$P, j≠i.

Voronoi diagrams identify regions of immediate influence in microstructures.
The representation of Voronoi regions in a microstructure facilitates the calculation of parameters as near neighbor distances and orientations, which are essential for the quantitative characterization of microstructures.

Statistical analysis by using Voronoi cells

Physical properties of heterogeneous materials are determined by the shapes, sizes and spatial distributions of the embedded particles. It is important to identify regular, nonregular, random, non-random or cluster patterns. Geometrical descriptors of the patterns are a powerful tool for the study of the physical properties of heterogeneous materials. The geometrical descriptors used for the Voronoi cell analysis are explained below.

Near Neighbor Distances (MNND). Mean distances between centers of inclusions that share a common Voronoi cell edge. It decreases with the clustering, especially at smaller area fractions.
Average Number of Near Neighbors (AVNUMR). An average number of inclusions that share a common Voronoi cell edge. The average number of near neighbors increases with the number of inclusions.

MNND is a very useful factor in determining the interaction between particles. The closest the particles are the higher the inter-particle effect. This geometrical factor will be used to determine the effect of the inter-particle interaction of composites fill in with carbon nanotubes. It will be used to determine if as Nan [21] suggested in his effective medium model the interaction between particles can be neglected for small volume fractions of particles.

The study of heterogeneous composites with Voronoi cells presents a powerful tool to study the clustering effect. During process fabrication, the filler particles tend to form clusters instead of presented a dispersed random distribution. Deviation from complete randomness is investigated through the ratio of the observed mean nearest neighbor distance to the expected mean for a purely random Poisson point distribution (MRNND) and the corresponding ratio of variances (VRNND). The expected mean and standard deviation of a purely Poisson distribution are calculated as [56]:

$$\text{Expected mean Poisson distribution} = 0.4\left(\frac{N}{A}\right)^{-1/2} \tag{30}$$

$$\text{Standard deviation of Poisson distribution} = \frac{4-\pi}{4\pi}\left[\frac{\frac{2}{N}}{A}\right] \tag{31}$$

where N/A is the density of inclusions.
Based on those ratios clusters on the heterogeneous materials can be identified according to the following criteria [56]:

MRNND	1	VRNND	1	Random set
MRNND	>1	VRNND	<1	Short-Range ordered sets
MRNND	<1	VRNND	<1	Clusters sets
MRNND	<1	VRNND	>1	Clusters with a superimposed background of random points

Voronoi cells are used in the present work to characterize carbon nanotubes based composites. The distance and a number of near neighbor distances are used as a tool to show the effect of the inter-particle interaction on the effective thermal conductivity of the composite.

Chapter 3. Simulations and Results.

3.1 Introduction.

The present study compares finite-element computations (FEA) and EMA model thermal conductivity estimation for CNT-matrix compositions with low to moderate volume fractions 0.001 to 0.02. The FEA results obtained showed that the EMA model underestimates the effective thermal conductivity of the composite when the particles are very close to each other, even for small particle volume fractions. EMA model assumes that for small volume fractions the fibers will be far away from each other and they do not interact. Small volume fraction does not necessarily means that the particles will be dispersed in the matrix, it is possible to have small volume fractions and embedded fibers close enough that they will interact with each other. For aligned fibers the Kapitza resistance cannot be neglected in the longitudinal direction. This study proposes a general correction function for the dependence on particle to particle interaction based on the near neighbor distances and the number of near neighbors.

3.2 Effective thermal conductivity characterization by FEA analysis.

The effective thermal conductivity of CNT-matrix composites is studied through FEA analysis. The model is constructed in 3D CAD software. It consists of 1, 3 or 5 CNT fibers aligned embedded in a silicon oil matrix. The dimensions of the fibers are specified in Table 2. The effective thermal conductivity of the fibers is calculated according to the EMA model. The matrix is silicon oil. It presents an isotropic thermal conductivity of 0.1 W/m K.

Table 2. *General properties of the CNT-composite.*

d(nm)	L (nm)	P=L/d	k_p (W/mK)	k_m (W/mK)	R_b (m^2 K/W)
20	2000	100	3000 [45]	0.1 [57]	2 E-8 [58]

d=diameter, **L**=length, **P**=aspect ratio, $\mathbf{k_p}$= thermal conductivity of the particle filler, $\mathbf{k_m}$=conductivity of the matrix, $\mathbf{R_b}$= Kapitza thermal resistance.

The matrix dimensions change from simulation to simulation. The length is in all the cases kept as twice of the fiber length and the width and depth are modified to obtain different CNT volume fractions. The fibers are centered in the silicon oil matrix domain. They occupy the 50% of the matrix length. The CNT fibers are at a distance of 25% of the total length to end wall boundary. The software used for the FEA analysis is ANSYS Mechanical. The orthotropic thermal conductivity of the fibers and the isotropic thermal conductivity of the matrix are manually specified in the software. The model used for the FEA analysis is shown in Figure 9. A temperature gradient is applied to the opposite faces of the matrix (faces A and B),

forcing the heat transfer through the longitudinal direction of the fiber. The other faces are considered adiabatic (faces C).
The number of nodes used for the FEA analysis for 1, 3 and 5 fibers as average is 150000, 300000 and 800000 respectively. A resolution study to determine if the mesh is fine enough was done. Increasing the number of nodes does not affect the final result.
The heat flux either in face A or B, shown in Figure 9 is estimated by the software. As faces C are considered adiabatic, by applying $\boldsymbol{Q/A = \Delta T/L/k}$ (32) the effective thermal conductivity can be calculated. Rearranging equation above the effective thermal conductivity estimated by FEA analysis is calculated as:

$$k_{FEA} = \frac{Q}{A}\frac{L_C}{\Delta T_{A-B}} \tag{33}$$

The thermal conductivity obtained through the FEA analysis corresponds to the overall system. The thermal resistance of the CNT-matrix composite can be seen in Figure 10. The total thermal resistance is the sum of three resistances in series. The thermal resistance due to the media, when there is no fibers and the equivalent thermal resistance in the presence of the fibers. The thermal resistance in the presence of the fibers captures the two-dimensional heat spreading at the end of the fibers and the conduction in parallel over the length. This last thermal resistance considerers the Kapitza resistance.

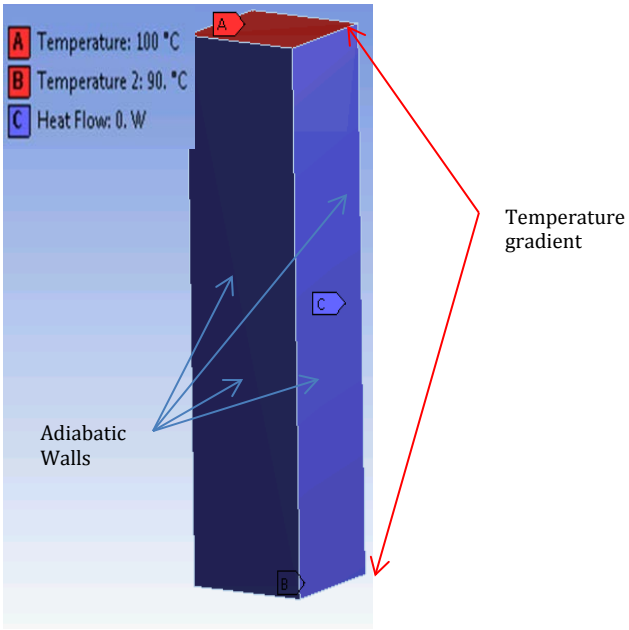

Figure 9. *Model schema for FEA analysis. Boundary conditions are 90 °C on the bottom, 100 °C on the top and zero heat flux at the walls.*

$$R_{TOTAL} = \frac{L_1}{k_m} + \frac{L_2}{k_{CNT-matrix}} + \frac{L_3}{k_m} = \frac{L_T}{k_T} \tag{34}$$

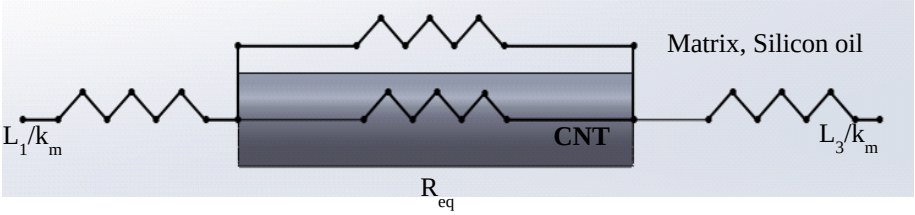

Figure 10. Thermal resistance analysis CNT-matrix system.

The FEA simulations predict the k_T, the thermal conductivity corresponding to the overall system. The EMA model predicts the thermal conductivity to the localized area where the fibers are embedded $k_{CNT\text{-}matrix}$. $L_1 = L_3 = ½\ L$ and L_2 is the length of the fiber, specified in Table 2. Equations 35-36 show the calculation of the thermal conductivities in the total matrix-CNT system and the thermal conductivities in the localized region where the fibers are embedded.

$$k_T = 2 * \left(\frac{k_m * k_{CNT-matrix}}{k_{CNT} + k_m}\right) \tag{35}$$

$$k_{CNT-matrix} = \frac{k_m * k_T}{2 * k_m - k_T} \tag{36}$$

3.2.1. Mesh quality evaluation.

The mesh is a discrete representation of the geometry to be studied. It designates different elements or cells where the equations will be approximated.
The mesh quality has an impact on the rate of convergence, solution accuracy and CPU time required. It is important to have a good mesh quality to achieve to an accurate and converged solution. The change in size from cell to cell shall be minimized. Differences in size between adjacent cells can result in not accurate results. The differential equations solved assume that the cells either grow or shrink smoothly.
The CPU time required is proportional to the number of elements. More elements require more time or slower solution. It is important to achieve a compromise of good mesh quality with a minimum number of cells.
The quality of the mesh will be measured based on two factors: Skewness and aspect ratio. The minimum number of cells required will be optimized by analyzing the impact on the results of the increment or decrement of the number of elements. When the increment of the number of cells does no impact on the result, it is concluded that the number of cells required to achieve to an accurate solution is enough.

Mesh quality

a. Skewness

Skewness measure how close is a cell to an ideal equilateral triangle or equiangular quad. The skewness factor goes from 1 poor quality to 0 excellent quality.
Highly skewed cells can be easily identified by visual inspection of the mesh. The software shows the quality of the mesh before running the simulation. Figure 12 shows the skewness of the cells for one single fiber embedded in the silicon matrix when the MNND with their mirror images is 100nm. Most of the cells present a skewness factor close to 0. This is a good indication that the mesh quality for the system to analyze is good enough, and the system can be solved.

Table 3. Skewness cell quality factor

Skewness	Cell Quality
1	Degenerate
0.9-<1	Bad
0.75-0.9	Poor
0.5-0.75	Fair
0.25-0.5	Good
>0-0.25	Excellent
0	Equilateral

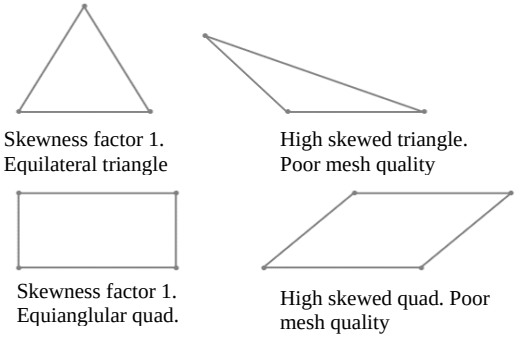

Figure 11. *Skewness mesh quality.*

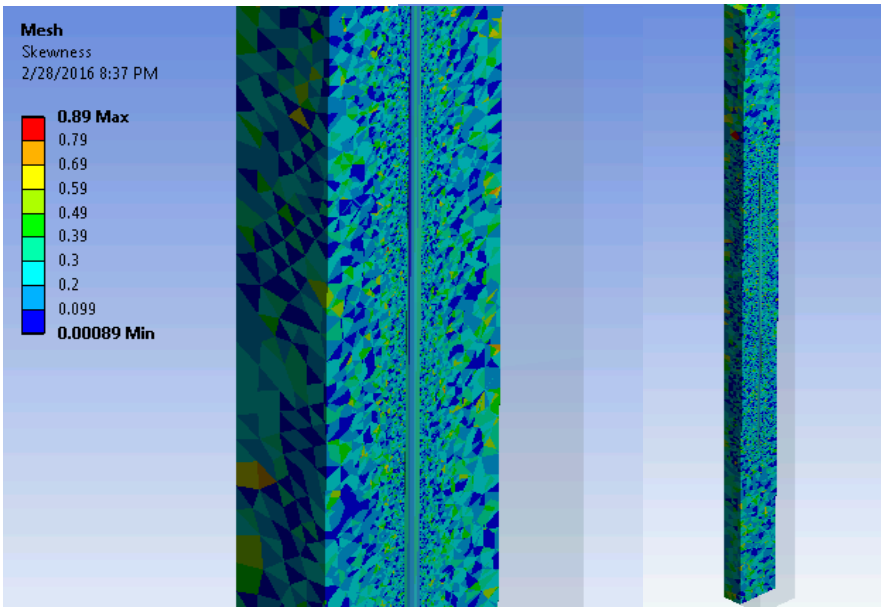

Figure 12. *Mesh quality by skewness factor. 1 fiber embedded in the matrix 100nm MNND.*

The skewness factor is analyzed for every simulation. When the quality of the cells is not good enough the meshing is modified until the skewness factor obtained is acceptable.

b. Aspect ratio

The aspect ratio is also an important factor to measure the quality of the mesh. It is defined as the ratio of longest edge length to the shortest edge length. An aspect ratio of 1 is a perfect meshing, 5-10 fair and higher than 20 is poor quality. As occurs with the skewness factor it can be inspected visually for a preliminary estimation of the quality of the mesh. The software indicates the quality of the mesh based on the aspect ratio. It is checked in every simulation. If bad cells are presented shall be modified until the quality of the mesh is acceptable.
Figure 14 shows the quality of cells based on the aspect ratio for one single fiber embedded in the matrix when the MNND with their mirror images is 100nm. Most of the cells present an aspect ratio close to 1. It is an indicative that the quality of the mesh is good.

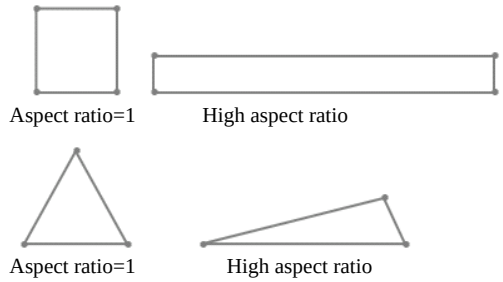

Figure 13. *Aspect ratio mesh quality*

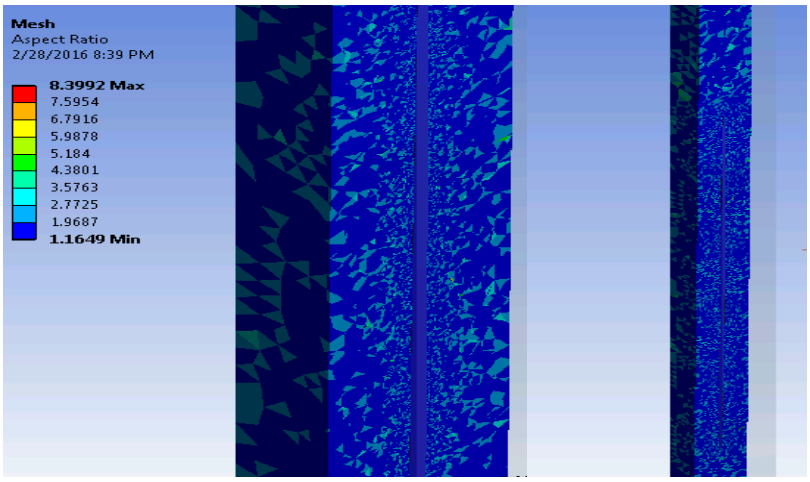

Figure 14. *Mesh quality by aspect ratio factor. 1 fiber embedded in matrix 100 nm MNND.*

Number of elements.

After achieving an acceptable mesh quality the number of elements needed to get an accurate solution without compromising the solver time is evaluated. The total thermal conductivity of the composite is evaluated for a different number of elements used in the mesh. The optimum value corresponds to the minimum

number of elements that gives accurate results. It means that if the number of elements is increased the result obtained does not change. Figure 16 shows the simulations done for the case of one single fiber embedded in a silicon matrix when the MNND with the mirror image is 100nm. Even though the difference is not much, it is possible to appreciate that after approximately 150000 elements the result remains the same. It can be concluded that for this case 150000 elements is the optimum number of elements.
As happened with the mesh quality, this analysis is repeated for every simulation. It is more tedious as the mesh quality inspection as requires running several simulations for each case. The average number of simulations required to find the optimum number of elements is 4.

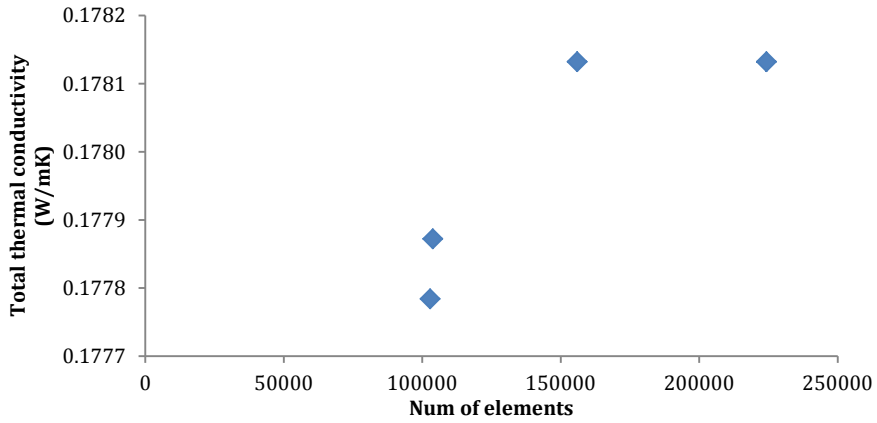

Figure 15. *Optimum number of elements required for one fiber embedded in a matrix when the MNND is 100nm.*

3.3. Effective thermal conductivity analysis for one fiber aligned. Correction factor proposed for EMA model.

Different cases are studied to evaluate the effective thermal conductivity prediction by the EMA model. The results predicted by the EMA model are compared with the results obtained by FEA simulations. Voronoi cells are used to characterize the distances between the particles by using the mean near neighbor distance and the number of particles that interact with a reference particle by the average number of near neighbors. One fiber aligned in the heat flux direction is studied. The results show that the Kapitza resistance cannot be neglected in the length direction. Not considering the Kapitza resistance leads to a notable overestimation of the thermal conductivity in the CNT-matrix region.
If the Kapitza resistance is considered, even for aligned fibers, the EMA model under predict the effective thermal conductivity compared to the FEA results in the cases studied. This deviation with the FEA results increases as the distances between particles decrease. Those results suggest that the interaction between particles may

have some effect on the effective thermal conductivity of the composite. A correction factor for the EMA model is proposed to account for the inter-particle interaction. This correction factor proposed is validated for different configurations.

3.3.1. One continuous aligned fiber. Without Kapitza resistance in the longitudinal direction.

One fiber aligned embedded in silicon oil matrix is studied to evaluate the thermal conductivity prediction of both models. Figure 9 and Figure 16 show the model set up used for FEA simulation. The fiber is centered in the matrix and the dimensions are specified in Table 2. The orthotropic thermal conductivity of the CNT is calculated according to Equations 20- 21. The EMA model estimates that in the length direction of the fiber the Kapitza resistance can be neglected.

Table 4 shows the thermal conductivity estimation by FEA analysis and EMA model for the total composite and the region where the fiber is localized. The total thermal conductivity by FEA analysis is obtained by software simulations and applying Equation 33. The thermal conductivity in the fiber-matrix region by FEA analysis is obtained by Equation 36 and using the total thermal conductivity obtained in the simulation. The thermal conductivity in the fiber-matrix region predicted by the EMA model is calculated according to Equation 23, where k_p is the thermal conductivity of the embedded particle. The total thermal conductivity of the composite predicted by the EMA model is calculated by Equation 35 and using the CNT-matrix thermal conductivity obtained by Equation 23. It is assumed that the fiber has 4 near neighbors. Each matrix boundary acts as a mirror projecting and identical image of 4 fibers surrounding. They interact with each other and through the symmetry at the boundary conditions with their reflected images.

The results show that the EMA model overestimates the effective thermal

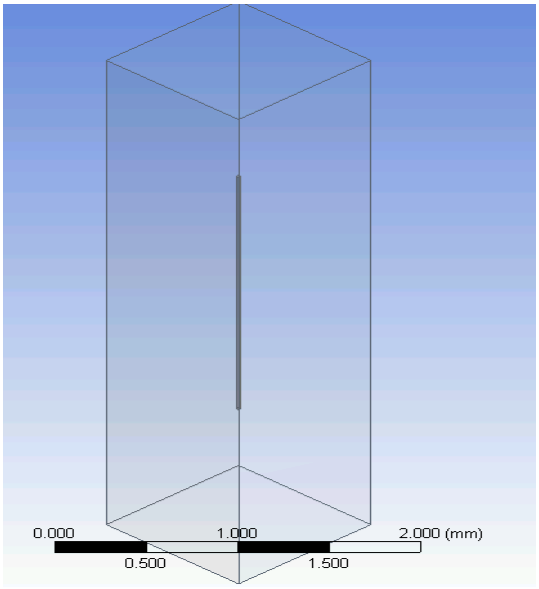

Figure 16. *1 fiber aligned embedded in a silicon oil matrix.*

conductivity in the CNT-matrix region. This overestimation increases notably as the distance between particles decreases. In case 10, where the particles are at a distance of 40 nm the EMA model predicts a thermal conductivity in the CNT-matrix region 15 times bigger than the FEA simulation. Figure 18 shows the prediction of the thermal conductivity by EMA model and FEA simulations as a function of the distance between the particles. As the distance between particles or mean near neighbor distance decreases the deviation between both models increases. The EMA model shows an exponential increase of the thermal conductivity as the distances between particles decreases while the FEA simulations present a linear increase of the thermal conductivity.

The results presented in this case suggested that the Kapitza resistance cannot be neglected in the length direction. As it can be appreciated in Figure 17 when the heat flux reaches one of the ends of the fiber is going to face some resistance due the interface CNT-matrix.

In the following cases, the Kapitza resistance will be considered in the length direction.

Table 4. *Morphology characterization by Voronoi cells and effective thermal conductivity estimation for one fiber aligned neglecting interface resistance in the length direction of the fiber.*

Case	***VF (%)***	***AN***	***MNND (nm)***	k_{T}***_FEA (W/mK)***	$k_{CNT\text{-}matrix}$***_FEA (W/mK)***	k_{T}***_EMA (W/mK)***	$k_{CNT\text{-}matrix}$***_EMA (W/mK)***	***Deviation CNT-matrix FEA-EMA (W/mK)***
1	0.015	4	500	0.1053	0.1112	0.1694	0.553	0.44
2	0.019	4	450	0.1264	0.1719	0.1736	0.658	0.49
3	0.023	4	400	0.1310	0.1898	0.1778	0.802	0.61
4	0.041	4	300	0.1432	0.2522	0.1860	1.327	1.07
5	0.080	4	200	0.1601	0.4008	0.1923	2.500	2.10
6	0.153	4	150	0.1701	0.5678	0.1958	4.700	4.13
7	0.345	4	100	0.1808	0.9395	0.1981	10.450	9.51
8	0.550	4	75	0.1862	1.3526	0.1988	16.599	15.25
9	1.000	4	50	0.1916	2.2844	0.1993	30.099	27.81
10	1.570	4	40	0.1937	3.0606	0.1996	47.198	44.14

VF*=volume fraction,* ***AN****=average number of near neighbors,* ***MNND****=mean near neighbor distance from wall fiber to wall fiber neighbor,* k_{T}***_FEA****= Total thermal conductivity by FEA analysis,* $k_{CNT\text{-}matrix}$***_FEA****= Fiber-matrix region thermal conductivity based on FEA analysis,* k_{T}***_EMA****= Total thermal conductivity by EMA model,* $k_{CNT\text{-}matrix}$***_EMA****= Fiber-matrix region thermal conductivity based on EMA model,* ***deviation****= deviation estimated thermal conductivity fiber-matrix region between FEA and EMA.*

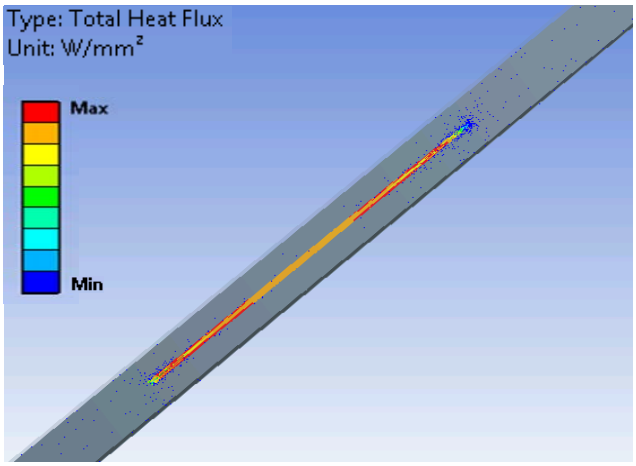

Figure 17. *Heat flux(W/mm²) of one CNT fiber aligned embedded in silicon oil matrix. FEA simulation.*

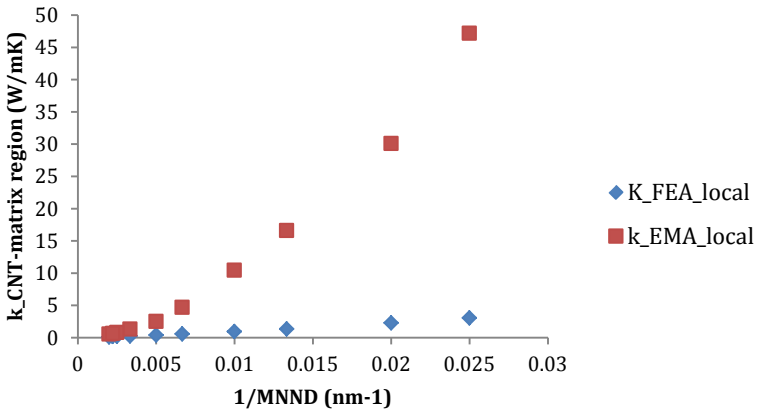

Figure 18. Thermal conductivity CNT-matrix region/ distance between particles variation by EMA and FEA models.

3.3.2. One continuous aligned fiber. Kapitza resistance in the longitudinal direction.

The results obtained for one fiber aligned neglecting the Kapitza resistance in the length direction showed the importance of this factor on the effective thermal conductivity. In the EMA model, the Kapitza resistance is added by changing the effective conductivity in the length direction according to the model equations. The estimation of the thermal conductivity in the transverse and longitudinal direction for one single fiber is proposed to be calculated according to [45]:

$$k_{11}^{c} = \frac{k_p}{1+2\frac{a_k}{d}\frac{k_p}{k_{matrix}}} \quad (37)$$

$$k_{33}^{c} = \frac{k_p}{1+2\frac{a_k}{L}\frac{k_p}{k_{matrix}}} \quad (38)$$

The equations above assume that the Kapitza resistance is affecting the thermal conductivity in all the directions.

One fiber aligned considering the Kapitza resistance in the length direction is studied. In this case, the distances between particles are smaller than in the previous case. It is intended to study the effect of the particles interaction in the effective thermal conductivity. The orthotropic thermal conductivity of the CNT-matrix region is calculated according to Equations 37-38. Same procedure as in the previous case is followed to estimate the thermal conductivities in the CNT-matrix and total composite by the EMA model and the FEA analysis. Table 5 shows the results obtained by both analyzes. The EMA model underestimates the thermal conductivity in the fiber-matrix region. This underestimation increases as the MNND increases, meaning that the particles are closer. When the particles are very close to each other as in case 1, 15nm mean near neighbor distances, the thermal conductivity predicted by the FEA analysis in the CNT-matrix region is almost 1.4 times bigger than the predicted by the EMA model. For the cases where the particles are further apart, as case 10, the thermal conductivity predicted by both methods is very similar. These values suggest that the interaction between particles may have some effect on the thermal conductivity even for small volume fractions

Table 5. *Morphology characterization by Voronoi cells and effective thermal conductivity estimation for one fiber aligned assuming interface resistance in the longitudinal direction of the fiber.*

Case	***VF (%)***	***AN***	***MNND (nm)***	k_{T}***_FEA (W/mK)***	$k_{CNT\text{-}matrix}$***_FEA (W/mK)***	k_{T}***_EMA (W/mK)***	$k_{CNT\text{-}matrix}$***_EMA (W/mK)***	***Deviation CNT-matrix FEA-EMA (W/mK)***
1	12.8	4	15	0.1978	8.8127	0.1969	6.3995	2.4131
2	9.82	4	20	0.1970	6.5313	0.1960	4.9216	1.6097
3	6.28	4	30	0.1952	4.0771	0.1939	3.1835	0.8936
4	4.35	4	40	0.1932	2.8343	0.1914	2.2359	0.5984
5	3.20	4	50	0.1910	2.1124	0.1887	1.6712	0.4412
6	2.45	4	60	0.1886	1.6501	0.1857	1.3030	0.3471
7	1.94	4	70	0.1861	1.3347	0.1826	1.0525	0.2822
8	1.64	4	80	0.1839	1.1422	0.1801	0.9052	0.2370
9	1.09	4	100	0.1781	0.8132	0.1728	0.6355	0.1777
10	0.51	4	155	0.1636	0.4495	0.1558	0.3520	0.0974

VF*=volume fraction,* ***AN****=average number of near neighbors,* ***MNND****=mean near neighbor distance,* k_{T}***_FEA****= Total thermal conductivity by FEA analysis,* $k_{CNT\text{-}matrix}$***_FEA****= Fiber-matrix region thermal conductivity based on FEA analysis,* k_{T}***_EMA****= Total thermal conductivity by EMA model,* $k_{CNT\text{-}matrix}$***_EMA****= Fiber-matrix region thermal conductivity based on EMA model,* ***deviation****= deviation estimated thermal conductivity fiber-matrix region between FEA and EMA.*

3.3.3. Correction factor for EMA model.

Based on the results obtained in *Table 5*, a correction factor for the underestimation of the EMA model is proposed. It is based on the MNND and the AN. It is meant to account for the inter-particle interaction effect on the thermal conductivity of CNT composites. It is assumed that the corrected thermal conductivity predicted by the EMA model can be expressed as:

$$k_{CNT-matrix\_EMAcorr} = k_{CNT-matrix,EMA} + k_{corr} \quad (39)$$

The correction factor estimation for one fiber aligned embedded in a matrix is shown Figure 19. It is based on the near neighbor distances and the average number of near neighbors of one particle filler in a Voronoi cell. Figure 19 shows the correction factor based on an AN of 4. It can be generalized and used for other cases diving by 4. The correction factor equation proposed to account for the inter-particle interaction is as follows

$$k_{corr} = \left(76.3\left(\frac{1}{MNND}\right)^2 + 4 * \frac{1}{MNND}\right) * \frac{1}{AN} \quad (40)$$

where MNND is the mean near neighbor distance for a particle in a Voronoi cell in nm, AN is the average number of near neighbors and *NT* is the total number of fibers in the composite. k_{corr} is the correction factor to be applied the EMA model in W/mK. The correction factor proposed in Equation (40) is used to reduce the underestimation of the thermal conductivity in the fiber-matrix region predicted by the EMA model.
In the following sections, this correction factor is evaluated for different configurations of three and five aligned fibers.

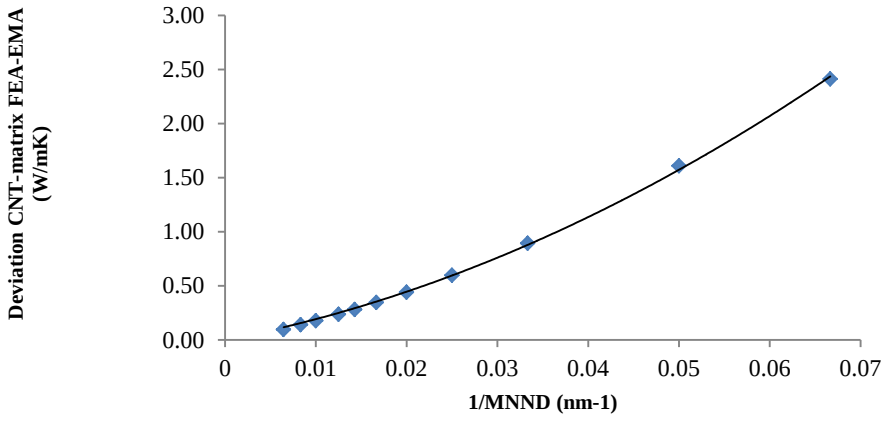

Figure 19. *Correction factor for the EMA model for one fiber aligned embedded in a silicon oil matrix.*

3.4. Characterization of the effective thermal conductivity by applying the correction factor to the EMA model.

The correction factor is derived from a simple geometry. It is, therefore, useful to test whether this approach will be accurate when more particle to particle interactions exist. The correction factor for the EMA model proposed in Equation 40 is evaluated for different configurations and compared to the results obtained by FEA analysis. It shall be noticed that this correction factor is applied to the thermal conductivity prediction by the EMA model in the CNT-matrix region.

The effective thermal conductivity obtained by FEA analysis is estimated by software simulations, as for the case of one single fiber. The orthotropic thermal conductivity of the CNT is estimated according to Equations 37-38. This thermal conductivity is used in the software to estimate the thermal conductivity predicted by FEA analysis in the CNT-matrix region and in the composite.

The effective thermal conductivity of the composite predicted by the EMA model is calculated based on Equations 22-23. The EMA model considers that the composite presents an orthotropic thermal conductivity. By the FEA analysis, the thermal conductivity obtained is calculated based on the direction of the heat flux. To be able to compare results with both approaches just Equation 23 is used as the effective thermal conductivity of the composite predicted by the EMA model. The thermal conductivity in the length direction of the fiber predicted by the EMA model is calculated according to Equation 38. The correction factor is applied to this thermal conductivity. The total thermal conductivity of the composite is calculated based on the corrected EMA thermal conductivity in the CNT-matrix region.

Three fibers aligned, and two different configurations for five fibers aligned are analyzed to evaluate the accuracy of the correction factor proposed. The results showed that by applying this correction factor it is possible to reduce the underestimation of the EMA model prediction to within <3% in most of the cases.

3.4.1. Three fibers aligned

The effective thermal conductivity of three CNT embedded in a silicon oil matrix is analyzed to evaluate the accuracy of the thermal conductivity for three interacting fibers. They interact with each other and through the symmetry at the boundary conditions with their reflected images. As it is was shown for the case of one fiber, even if the fibers are aligned in the direction of the heat flux, the interface resistance in the longitudinal direction of the fibers and the matrix cannot be neglected. Figure 20 a)-b) presents the model schema used for the FEA analysis. Figure 20 c) shows a Voronoi cell diagram for the three fibers. In this case, each fiber will have 2 near neighbors and the distance between near neighbors is specified by NDD_i. NDD_i is the distance between fibers center.

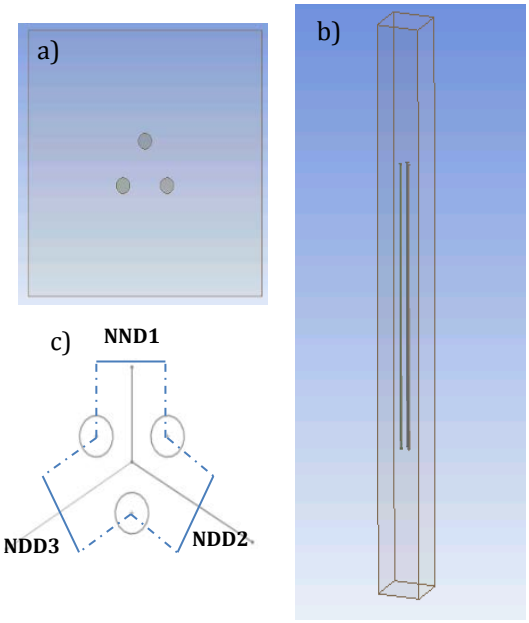

Figure 20. *(a) and (b) 3 fibers aligned embedded in a silicon oil matrix. (c) Voronoi cell for the three fibers contained in the matrix.*

For this case, their reflected images are not considered near neighbors. The distance of the fibers to the matrix walls is 2*NDDmax. They are far enough to not be considered near neighbors. The results obtained for the 3 fibers case are shown in Table 6. The EMA model underestimates the effective thermal conductivity of the fiber-matrix region. This underestimation increases as the distances between the particles decreases. When the fibers are 150 nm apart the EMA model predicts an effective thermal conductivity very similar to the FEA analysis. But for the case of 40 nm, the difference between the FEA and the EMA is notable. The deviation between the FEA values and the EMA values increases as the NND decreases, with deviations between 7-15% for the cases presented. The thermal conductivity prediction on the fiber-matrix region by applying the correction factor reduces the deviation of the EMA model to within < 7% in most of the cases.

For the last two cases, when the fibers are 30 and 25 nm apart, the particles are very close to each other, forming a cluster. The effective thermal conductivity predicted by applying the correction factor estimates a thermal conductivity not as accurate as for the other cases. The effect of the clustering may have some effect on the effective thermal conductivity that the correction factor proposed is not considering.

The total thermal conductivity prediction by applying the correction factor is very close to the predicted by the FEA model. It reduces the EMA under prediction to within < 2% in all the cases where there are no clusters. The total thermal conductivity describes the heat transfer per unit length in the fibers-matrix region and also the regions of the composite where there are no fibers.

As it is shown in the results for the three fibers case, the application of the correction factor improves the effective thermal conductivity predicted by the EMA model until the clustering effect has an important effect on the thermal conductivity.

Table 6. *Morphology characterization by Voronoi cells and effective thermal conductivity estimation for three fiber aligned assuming interface resistance in the longitudinal direction of the fibers.*

Case	*VF (%)*	*AN*	*NND1 -3 (nm)*	k_T *FEA (W/mK)*	$k_{CNT\text{-}matrix}$ *FEA (W/mK)*	$k_{CNT\text{-}matrix}$ *EMA (W/mK)*	$k_{CNT\text{-}matrix}$ *EMA corrected (W/mK)*	k_T *EMA corrected (W/mK)*
1	0.08	2	150	0.1221	0.1568	0.1393	0.1562	0.1219
2	0.18	2	100	0.1375	0.2200	0.1884	0.2163	0.1368
3	0.41	2	65	0.1564	0.3587	0.3013	0.3505	0.1556
4	1.00	2	40	0.1744	0.6825	0.5910	0.6893	0.1747
5	1.67	2	30	0.1821	1.0198	0.9200	1.0722	0.1829
6	2.29	2	25	0.1859	1.3168	1.2195	1.4225	0.1869

VF*=volume fraction,* ***AN****=average number of near neighbors,* ***NND****=near neighbor distance,* k_T***_FEA****= Total thermal conductivity by FEA analysis,* ***k_CNT-matrix_FEA****= thermal conductivity fiber-matrix region by FEA analysis,* ***k_CNT-matrix_EMA****= thermal conductivity fiber-matrix region by EMA model,* ***k_CNT-matrix_EMA corrected****= thermal conductivity fiber-matrix region by EMA model applying correction factor,* k_T***_EMA corrected****= total thermal conductivity by EMA model applying correction factor,*

3.4.2. Five fibers aligned. Configuration 1

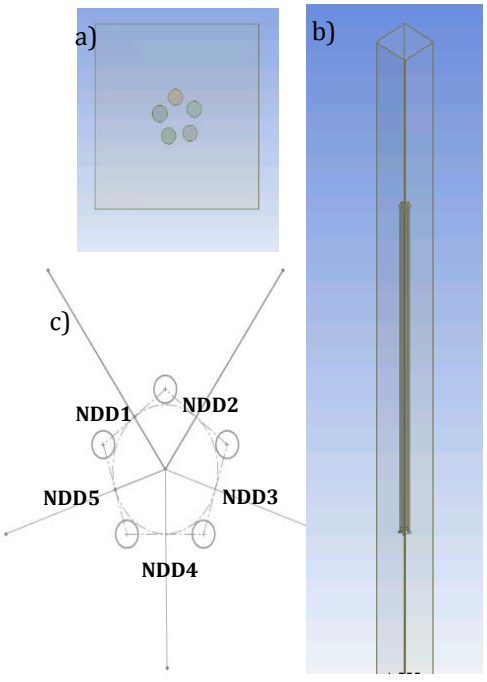

Figure 21. *(a) and (b) 5 fibers aligned embedded in a silicon oil matrix. (c) Voronoi cell for the five fibers contained in the matrix.*

The effective thermal conductivity of five CNT fibers aligned embedded in a silicon oil matrix is also evaluated. The model used for the FEA analysis is shown in Figure 21 a) and b) and Figure 21 c) represents the schema of a Voronoi cell. In this case, each fiber will have two near neighbors and the distance between them is specified by NND_i. The distances NND_i for all the cases analyzed are specified in Table 7. Their reflected images are not considered near neighbors. The distance between fibers and matrix is 2*NDDmax. They are far enough to considerer that they do not interact. As for three fibers aligned case, the deviation on the thermal conductivity prediction increases as the distance between the fibers decreases. When no correction factor is applied the effective thermal conductivity predicted by the EMA model on the fiber-matrix region differs from 10-13% in most of the cases with the FEA analysis. By applying the correction factor to the EMA model, the local error is reduced to within <5%. The deviation of the total thermal conductivity prediction is <3% for all the cases.

When the particles are very close to each other, as in case 6, the correction factor proposed predicts accurately the effective thermal conductivity in the fiber-matrix region. In this particular case, it seems that the clustering is not affecting the effective thermal conductivity.

For this particular configuration of five fibers aligned, the application of the correction factor proposed improves the thermal conductivity prediction of the EMA model.

Table 7. *Morphology characterization by Voronoi cells and effective thermal conductivity estimation for five fibers aligned assuming interface resistance in the longitudinal direction of the fibers.*

Case	***VF (%)***	***AN***	***NND1 -5(nm)***	k_T ***FEA (W/mK)***	$k_{CNT\text{-}matrix}$ ***FEA (W/mK)***	$k_{CNT\text{-}matrix}$ ***EMA (W/mK)***	$k_{CNT\text{-}matrix}$ ***EMA corrected (W/mK)***	k_T ***EMA corrected (W/mK)***
1	0.11	2	150	0.1280	0.1779	0.1540	0.1709	0.1262
2	0.29	2	100	0.1488	0.2906	0.2444	0.2722	0.1460
3	0.46	2	70	0.1603	0.4043	0.3259	0.3704	0.1575
4	0.87	2	50	0.1717	0.6061	0.5272	0.5982	0.1714
5	1.32	2	40	0.1784	0.8268	0.7481	0.8464	0.1789
6	2.2	2	30	0.1857	1.2998	1.1802	1.3325	0.1860

VF*=volume fraction,* ***AN****=average number of near neighbors,* ***NND****=near neighbor distance,* k_T***_FEA****= Total thermal conductivity by FEA analysis,* ***k_CNT-matrix_FEA****= thermal conductivity fiber-matrix region by FEA analysis,* ***k_CNT-matrix_EMA****= thermal conductivity fiber-matrix region by EMA model,* ***k_CNT-matrix_EMA corrected****= thermal conductivity fiber-matrix region by EMA model applying correction factor,* k_T***_EMA corrected****= total thermal conductivity by EMA model applying correction factor,*

3.4.3. Five fibers aligned. Configuration 2

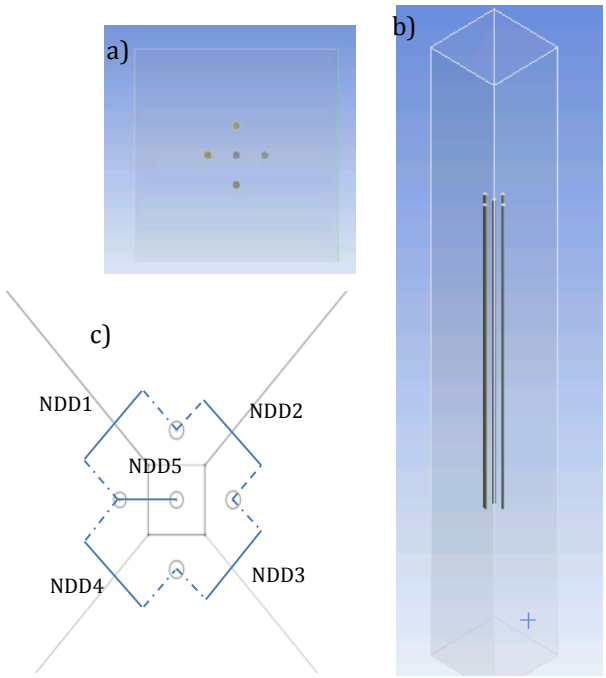

Figure 22. *(a) and (b) 5 fibers aligned embedded in a silicon oil matrix. (c) Voronoi cell for the five fibers contained in the matrix.*

A second configuration of five fibers aligned is studied. It is important to understand how the different disposition of the fibers affects the effective thermal conductivity of the composite. The configuration used is shown in Figure 22. Figure 22 a) and b) show the 3D model used in the FEA software and Figure 22 c) the Voronoi diagram corresponding to this configuration. It is important to notice that in this configuration there is one fiber surrounding for the other four. This fiber in the middle is going to interact with all the other fibers.

In Table 8 the results obtained for different near neighbor distances are presented. Their reflected images are not considered as near neighbors. The distance of the fibers to the matrix walls is 2*NDDmax. They are far enough to not be considered near neighbors.

In this case, no trend is observed. The deviation of the EMA model prediction is similar in most of the cases. It is not increasing as the distance between particles decreases as it happened in the other cases. The EMA model prediction in the fiber-matrix region when no correction factor is applied differs by 11-16% in most of the cases. The application of the correction reduces this deviation to <7% in the fiber-matrix region in most of the cases and to <2% for the total effective thermal conductivity of the composite.

Case number 6, where the distance between fibers is 40 and 30 nm, the thermal conductivity estimation on the fiber-matrix region by applying the correction factor differs 8% compared to the predicted by the FEA analysis. The effect of the

clustering may have some effect on the effective thermal conductivity that the correction factor proposed does not consider.

Table 8. *Morphology characterization by Voronoi cells and effective thermal conductivity estimation for five fibers aligned (configuration 2) assuming interface resistance in the longitudinal direction of the fibers.*

Case	***VF (%)***	***AN***	***NND1 -4(nm)***	***NND5 (nm)***	k_T ***FEA (W/mK)***	$k_{CNT\text{-}matrix}$ ***FEA (W/mK)***	$k_{CNT\text{-}matrix}$ ***EMA (W/mK)***	$k_{CNT\text{-}matrix}$ ***EMA corrected (W/mK)***	k_T ***EMA corrected (W/mK)***
1	0.14	3	150	105	0.1329	0.1981	0.1687	0.1823	0.1292
2	0.23	3	130	90	0.1380	0.2226	0.2129	0.2294	0.1393
3	0.31	3	100	70	0.1488	0.2906	0.2522	0.2757	0.1468
4	0.61	3	70	50	0.1637	0.4510	0.3995	0.4385	0.1629
5	0.86	3	60	40	0.1715	0.6023	0.5223	0.5728	0.1703
6	1.59	3	40	30	0.1804	0.9181	0.8807	0.9719	0.1813

VF*=volume fraction,* ***AN****=average number of near neighbors,* ***NND****=near neighbor distance,* k_T***_FEA****= Total thermal conductivity by FEA analysis,* ***k_CNT-matrix_FEA****= thermal conductivity fiber-matrix region by FEA analysis,* ***k_CNT-matrix_EMA****= thermal conductivity fiber-matrix region by EMA model,* ***k_CNT-matrix_EMA corrected****= thermal conductivity fiber-matrix region by EMA model applying correction factor,* k_T***_EMA corrected****= total thermal conductivity by EMA model applying correction factor,*

Chapter 4. Results discussion and conclusions.

CNT are very promising materials to be used as thermal interface materials. Thermal interface materials facilitate a pathway for heat to be transferred from the chip to the heat dissipation device. Improvement of thermal interface materials shall reduce costs associated with cooling devices. The thermal conductivity of a thermal interface material depends on the bond line thickness, the contact resistance between the thermal interface material and contacting surfaces and the thermal conductivity of the bulk material. By using materials with high thermal conductivity, the contact resistance is minimized between components facilitating a pathway for the heat to be transferred.

There are many theoretical and empirical relations to predict the thermal conductivity of solid filled composites. Most of those theoretical models do not include the interfacial resistance on the particle/matrix surface. The interfacial contact resistance is associated with the combination of poor mechanical or chemical adherence at the interface or a thermal expansion mismatch between the particle and the matrix. The interface contact resistance plays an important role at nanoscale heat transfer. The thermal resistance of the interface CNT-silicon oil matrix is 2 E-8 m^2 K/W [58]. This interface resistance reduces 98% the effective thermal conductivity in the longitudinal direction of the fiber. The EMA model proposed by Nan can predict the effective thermal conductivity of randomly dispersed long fibers for a very low volume fraction($f<0.01$). This theory is based on some assumptions that are questionable. It considers that for very low volume fraction of fillers, the particles are dispersed in the matrix and do not interact with each other. It also assumes that for fibers aligned in the heat flux direction the interface resistance can be neglected in the fiber longitudinal direction. In the present work, those assumptions are shown to be not completely valid.

The present work compares FEA computations and EMA thermal conductivity estimation for CNT-matrix with low to moderate volume fraction. The FEA modeling considers the thermal conductivity of the fiber and the Kapitza resistance. For the case of one fiber aligned, the results presented show that neglecting the thermal interface resistance in the length direction can overestimate the effective thermal conductivity in the CNT-matrix region by 1500 % when the fibers are close to the near neighbors. The overestimation increases as the distance between fibers decreases. The thermal conductivity is much higher in the length direction than in the radial direction of the fiber, but when the heat flux approached the fibers ends are going to face a high thermal resistance due to the interface CNT-silicon oil matrix. The interface resistance shall be considered in all three directions even for aligned fibers.

Voronoi cells are used in the present work to characterize carbon nanotubes based composites. The distance and a number of near neighbor distances are used as a tool to show the effect of the inter-particle interaction on the effective thermal conductivity of the composite. For closely packed particle the use of MNND is suggested. The EMA model underestimates the effective thermal conductivity compared to the results obtained through FEA analysis. This underestimation

increases as the MNND decreases, meaning that the particles are closer. It is proposed a correction factor based on the MNND and the AN to account for the inter-particle interaction.

The results obtained show that even for small volume fractions, the EMA model underestimates the effective thermal conductivity of the CNT composite. For the case of 3 fibers aligned when the MNDD is 100 nm the EMA, the model predicts an effective thermal conductivity in the CNT-matrix region 80% less than the FEA analysis. The underestimation increases as the distance between particles decreases. If the correction factor proposed is applied the effective thermal conductivity on the CNT-matrix region estimation only differs <5% in most of the cases. The fact that the fibers are forming clusters is believed that have some effect on the thermal conductivity, as it is manifested by the results obtained for three fibers aligned when they are 30nm and 25nm far apart. The correction factor proposed does not consider the effect that clusters may cause in the thermal conductivity. Further studies must be done to analyze the effect of clusters on the effective thermal conductivity of nanocomposites. The model predicts very accurately the effective thermal conductivity of the composite within a precision of <1% for all the cases.

For the five fibers case, when the fibers are disposed of in a pentagonal configuration as occurs for the three fibers, as the MNND decreases the deviation with the FEA model increases. In this case, when the fibers were very close to each other forming clusters no effect was observed on the thermal conductivity. According to the Voronoi diagram, the number of near neighbors for each fiber is two. If the fibers are very close to each other, forming a cluster, the number of near neighbors in one filler can increase. The further analysis shall be carried to study the effect of clustering in this configuration. By applying the correction factor to the EMA model, the thermal conductivity in the CNT-matrix region predicted differs <7% with the FEA results. The deviation of the composite thermal conductivity prediction is <2% for all the cases.

In the configuration 2, for five fibers aligned, the increase of the EMA model deviation as the distance between particles decreases was not observed. For this particular case, the clusters formation may have an important effect. The EMA model prediction in the fiber-matrix region when no correction factor is applied differs by 11-16% in most of the cases. The application of the correction reduces this deviation to <7% in the fiber-matrix region in most of the cases and to <2% for the total effective thermal conductivity of the composite.

This work proposes a correction factor to account for the inter-particle interaction in the EMA model. It is based on the NDD and the AN on a representative Voronoi cell in the composite. It reduces the underestimation of the total conductivity of the EMA model to within an error < 3% in most of the cases.

Acknowledgments.

I would like to thank my advisor Dr. Drazen Fabris for his excellent guidance, dedication, and support. Thanks for making this research possible, it has been an excellent experience working with you.

I would also like to thank Dr. On Shun Pak as the second reader of this thesis. I am very grateful of your participation on this thesis.

Calvin Tszeng, thanks for the suggestion to use Voronoi cells. It was a very valuable input for this work.

Thanks to Lantz Johnson and Jason Chong for their efficient assistance on software related problems.

I want to thank my parents and brother for your unconditional support.

Finally, I want to thank Roberto for his support and encouragement throughout my years in Santa Clara. This challenging journey would not have been possible without you.

Appendix.

Appendix A: Mesh quality.

In section 3.2.1 it was explained how the mesh quality is evaluated for one fiber embedded in the matrix. The example showed corresponds to the case when the MNND is 100nm. The method described to optimizing the mesh is done for every simulation. In this section, the same example for three fibers and five fibers is shown when MNND is 100nm.

3 cylinders MNND 100nm

Figure 23 shows the skewness factor and aspect ratio for the three fibers configuration when the MNND is 100nm. The figure on the left shows the skewness factor. Most of the cells present a skewness factor close to 0. The figure on the right shows the aspect ratio of the cells. The majority of the cells have an aspect ratio 1-2. Figure 24 show the optimum number of elements for the example presented. 200000 cells are sufficient to achieve to an accurate solution.

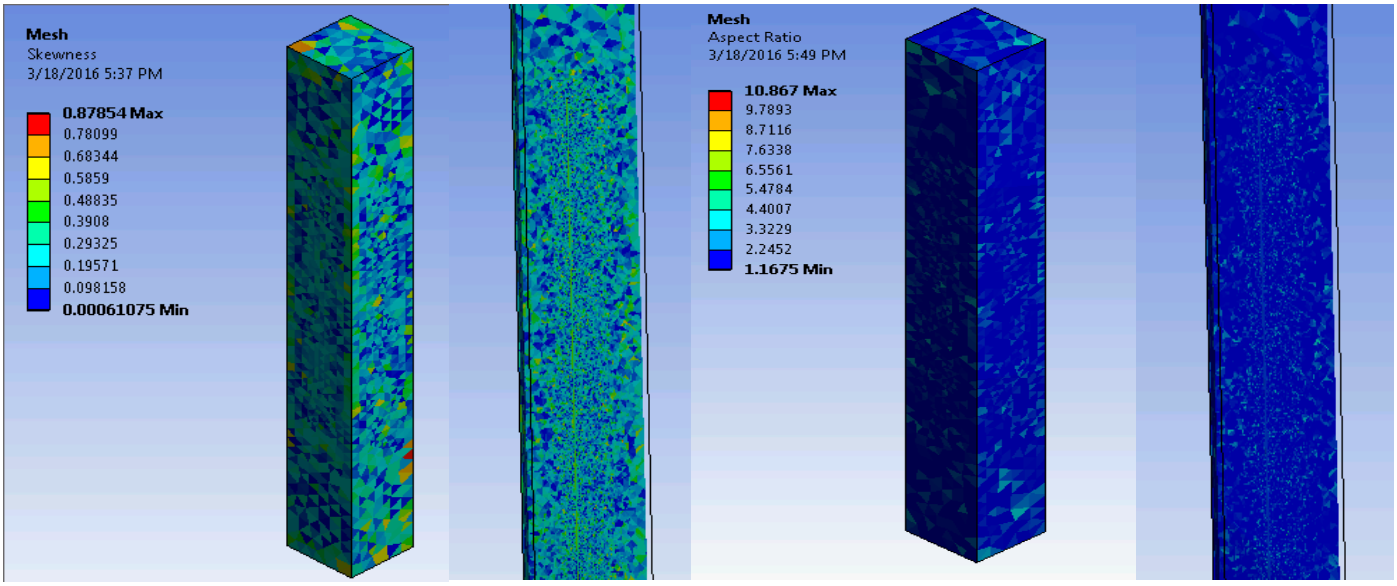

Figure 23. Mesh quality for 3 cylinders with MNND 100 nm. Left figure skewness factor, isometric view and cross section where the fiber is located. Right figure aspect ratio, isometric view and cross section where the fiber is located.

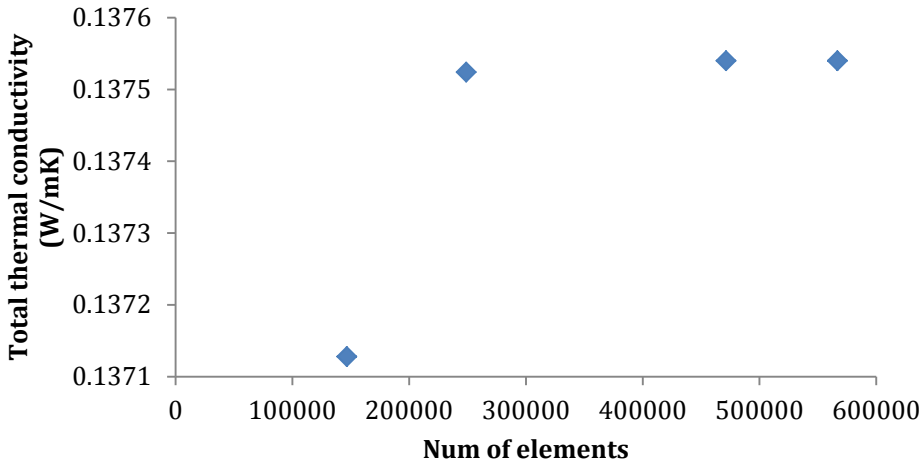

Figure 24. *Optimum number of elements required for three fibers embedded in a matrix when the MNND is 100nm.*

5 cylinders MNND 100nm. Configuration 1

Figure 25 shows the mesh quality for five cylinders distributed in a pentagonal configuration when the MNND is 100nm. Figure 26 shows the estimation of the optimum number of elements to obtain an accurate solution. As happened in previous cases, the variation is very small by increasing the number of cells when the mesh quality determined by the skewness and aspect ratio is good enough. Even though, it can be concluded that 800000 cells are the optimum number of cells to achieve to an accurate solution.

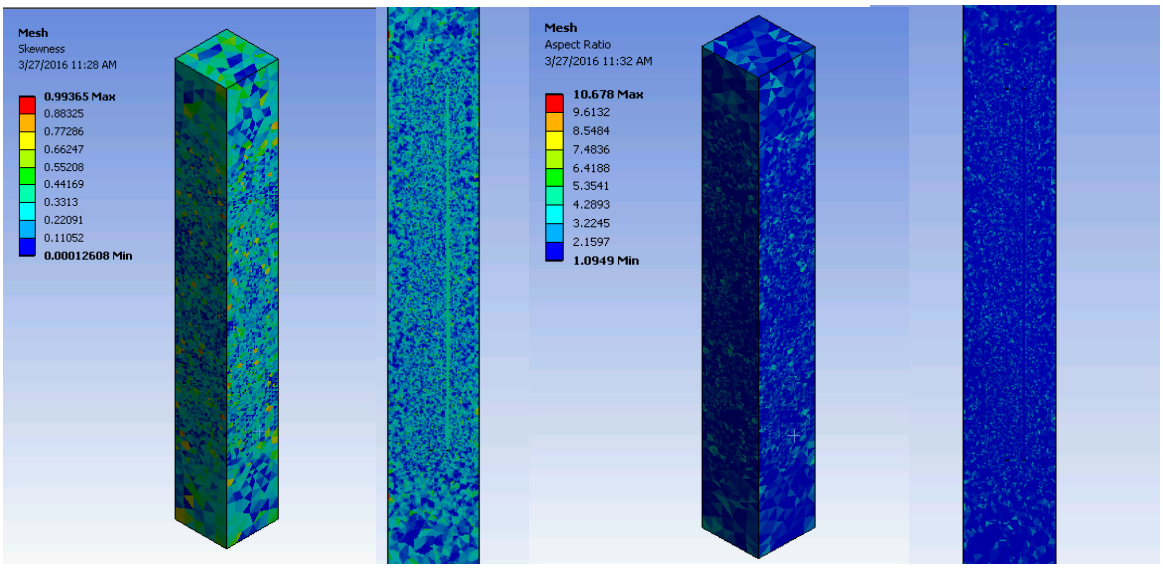

Figure 25. *Mesh quality for 5 cylinders with MNND 100 nm in pentagonal configuration. Left figure skewness factor, isometric view and cross section where the fiber is located. Right figure aspect ratio, isometric view and cross section where the fiber is located.*

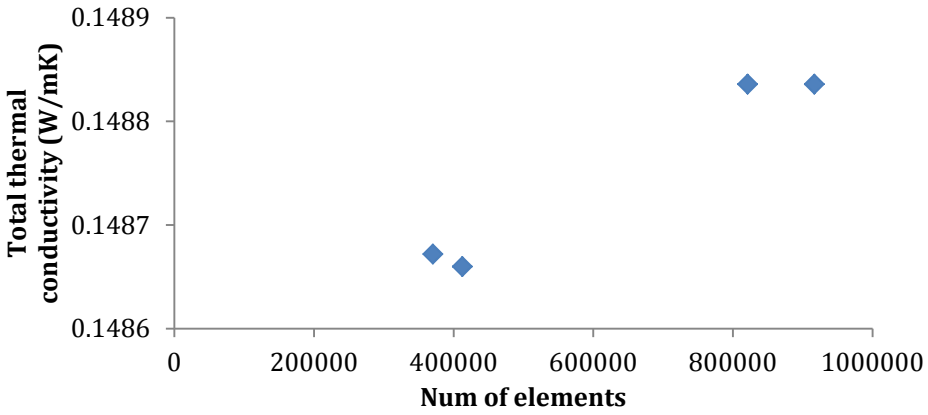

Figure 26. *Optimum number of elements required for five fibers embedded in a matrix in a pentagonal distribution when the MNND is 100nm.*

5 cylinders MNND 100nm. Configuration 2

Figure 27 shows the mesh quality for five fibers embedded in a matrix in a circular configuration. On the left side is shown the skewness factor. There are some bad cells in the matrix region. In the cross section view, where the fiber is embedded the majority of the cells present a skewness factor close to zero. The aspect ratio is close to 1 in most of the cells. Figure 28 show the estimation of the optimum number of cells required to achieve to an accurate solution. It is concluded that 800000 is the optimum number of cells.

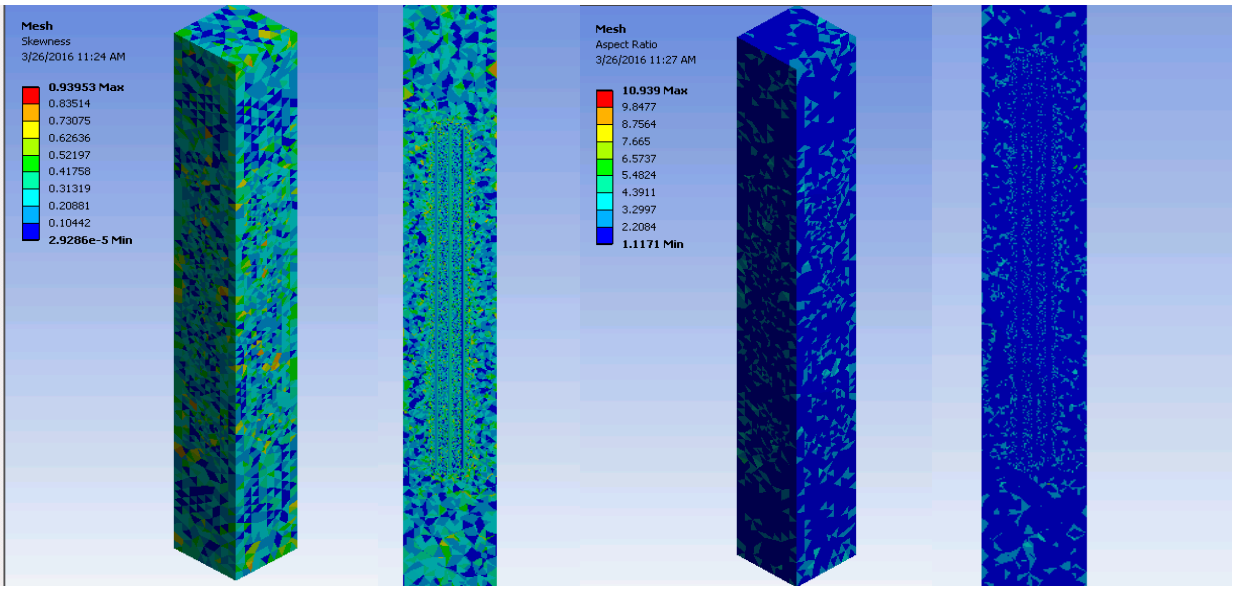

Figure 27 *Mesh quality for 5 cylinders with MNND 100 nm in circular configuration. Left figure skewness factor, isometric view and cross section where the fiber is located. Right figure aspect ratio, isometric view and cross section where the fiber is located.*

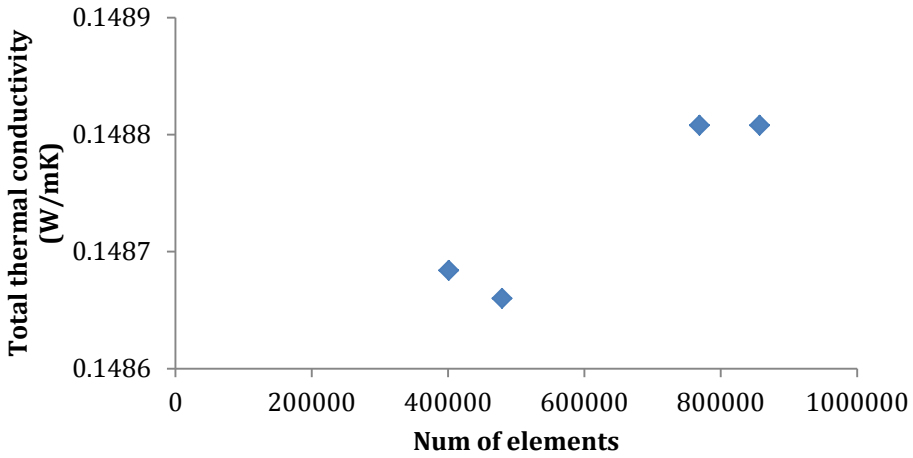

Figure 28. *Optimum number of elements required for five fibers embedded in a matrix in a circular distribution when the MNND is 100nm.*

Appendix B: Correction factor as sum of interactions

A different approach estimating the correction factor to the one explained above has been analyzed. It is based on the results obtained in *Table 6*. It depends on the NND_i between fibers and the AN. The correction factor estimation for one fiber aligned embedded in a matrix is shown Figure 20. Figure 20 shows the correction factor based on an AN of 4. It can be generalized and used for other cases diving by the number of AN. The correction factor equation proposed to account for the inter-particle interaction is as follows

$$k_{corr} = \sum_{i=1}^{AN}(76.33\left(\frac{1}{NND_i}\right)^2 + 4.04\frac{1}{NND_i}) \quad (41)$$

The corrected thermal conductivities for the cases of three and five fibers are presented below. The corrected thermal conductivity predicted by this method present a higher deviation with respect to the FEA thermal conductivity. For this reason, this method was discarded.

Three fibers aligned

The results presented in Table 9 can be compared with Table 6. The method base on Equation 41 estimates the effective thermal conductivity in the matrix-fiber region with a higher error.

Table 9. *Morphology characterization by Voronoi cells and effective thermal conductivity estimation for three fiber aligned. Correction factor estimated according to Equation 41*

Case	***VF (%)***	***AN***	***NND1 -3 (nm)***	k_T ***FEA (W/mK)***	$k_{CNT\text{-}matrix}$ ***FEA (W/mK)***	$k_{CNT\text{-}matrix}$ ***EMA (W/mK)***	$k_{CNT\text{-}matrix}$ ***EMA corrected (W/mK)***	k_T ***EMA corrected (W/mK)***
1	0.08	2	150	0.1221	0.1568	0.1401	0.1704	0.1260
2	0.18	2	100	0.1376	0.2203	0.1884	0.2365	0.1406
3	0.41	2	65	0.1564	0.3587	0.3013	0.3816	0.1585
4	1.00	2	40	0.1744	0.6825	0.5910	0.7398	0.1762
5	1.67	2	30	0.1821	1.0198	0.9200	1.1396	0.1839
6	2.29	2	25	0.1859	1.3168	1.2244	1.5083	0.1876

VF*=volume fraction,* ***AN****=average number of near neighbors,* ***NND****=near neighbor distance,* k_T***_FEA****= Total thermal conductivity by FEA analysis,* ***k_CNT-matrix_FEA****= thermal conductivity fiber-matrix region by FEA analysis,* ***k_CNT-matrix_EMA****= thermal conductivity fiber-matrix region by EMA model,* ***k_CNT-matrix_EMA corrected****= thermal conductivity fiber-matrix region by EMA model applying correction factor,* k_T***_EMA corrected****= total thermal conductivity by EMA model applying correction factor,*

Five fibers aligned. Configuration 1

As happened for the three fibers case, the method base on Equation 41 presents a higher error on the thermal conductivity estimation. The results show in Table 10 can be compared with the results presented in Table 7.

Table 10. *Morphology characterization by Voronoi cells and effective thermal conductivity estimation for five fibers aligned. Correction factor estimated according to Equation 41*

Case	***VF (%)***	***AN***	***NND1 -5(nm)***	k_T ***FEA (W/mK)***	$k_{CNT\text{-}matrix}$ ***FEA (W/mK)***	$k_{CNT\text{-}matrix}$ ***EMA (W/mK)***	$k_{CNT\text{-}matrix}$ ***EMA corrected (W/mK)***	k_T ***EMA corrected (W/mK)***
1	0.11	2	150	0.1280	0.1779	0.1540	0.1844	0.1297
2	0.29	2	100	0.1458	0.2690	0.2424	0.2905	0.1488
3	0.46	2	70	0.1603	0.4043	0.3259	0.3992	0.1599
4	0.87	2	50	0.1717	0.6061	0.5272	0.6386	0.1729
5	1.32	2	40	0.1784	0.8268	0.7481	0.8970	0.1799
6	2.2	2	30	0.1857	1.2998	1.1802	1.3998	0.1867

VF*=volume fraction,* ***AN****=average number of near neighbors,* ***NND****=near neighbor distance,* k_T***_FEA****= Total thermal conductivity by FEA analysis,* ***k_CNT-matrix_FEA****= thermal conductivity fiber-matrix region by FEA analysis,* ***k_CNT-matrix_EMA****= thermal conductivity fiber-matrix region by EMA model,* ***k_CNT-matrix_EMA corrected****= thermal conductivity fiber-matrix region by EMA model applying correction factor,* k_T***_EMA corrected****= total thermal conductivity by EMA model applying correction factor,*

Five fibers aligned. Configuration 2

Table 11 shows the results for the case of five aligned fibers configured in a circular shape. Those results can be compared to Table 8. The deviation between the thermal conductivity in the matrix-CNT region is higher in this configuration compared to the other two configurations presented. The reason for this high deviation can be related to the clustering effect. The fibers are distributed in a way that instead of just have three near neighbors the inter-particle effect may be higher if the particles are close enough.

***Table 11**. Morphology characterization by Voronoi cells and effective thermal conductivity estimation for five fibers aligned (configuration 2). Correction factor estimated according to Equation 41*

Case	***VF (%)***	***AN***	***NND1 -4(nm)***	***NND5 (nm)***	k_T ***FEA (W/mK)***	$k_{CNT\text{-}matrix}$ ***FEA (W/mK)***	$k_{CNT\text{-}matrix}$ ***EMA (W/mK)***	$k_{CNT\text{-}matrix}$ ***EMA corrected (W/mK)***	k_T ***EMA corrected (W/mK)***
1	0.14	3	150	105	0.1329	0.1981	0.1687	0.2019	0.1338
2	0.23	3	130	90	0.1380	0.2226	0.2129	0.2522	0.1432
3	0.31	3	100	70	0.1503	0.3027	0.2522	0.3052	0.1506
4	0.61	3	70	50	0.1637	0.4510	0.3995	0.4802	0.1655
5	0.86	3	60	40	0.1715	0.6023	0.5223	0.6242	0.1724
6	1.59	3	40	30	0.1804	0.9181	0.8807	1.0423	0.1825

***VF**=volume fraction, **AN**=average number of near neighbors, **NND**=near neighbor distance, **k_T_FEA**= Total thermal conductivity by FEA analysis, **k_CNT-matrix_FEA**= thermal conductivity fiber-matrix region by FEA analysis, **k_CNT-matrix_EMA**= thermal conductivity fiber-matrix region by EMA model, **k_CNT-matrix_EMA corrected**= thermal conductivity fiber-matrix region by EMA model applying correction factor, **k_T_EMA corrected**= total thermal conductivity by EMA model applying correction factor,*

List of References:

[1] E. Shein, "Keeping Computers Cool From the Inside," *Comunications of the ACM,* vol. 56, 2013.

[2] "Thermal Adhesivesm TIMs & Phase Change Materials," [Online]. [Accessed 11 10 2015].

[3] P. Garimella, *Cooling Technologies Research Center (CTRC),* 2014.

[4] F. P.Incropera, D. P. Dewitt, T. L. Bergman, A S. Lavin**e**, Fundamentals of Heat and Mass Transfer, Seventh Edition, John Wiley & Sons.

[5] R. Prasher, "Thermal Interface Materials: Historical Perspective, Status and Future Directions," *Proceedings of the IEEE,* pp. 1571-586, 2006.

[6] R. Prasher, J. Shipley, S. Prstic, P. Koning, J. Wang, "Thermal Resistance of Particle Laden Polymeric Thermal Interface Materials," vol. 125, pp 1170-1177, *ASME 2003 International Mechanical Engineering Congress and Exposition*. American Society of Mechanical Engineers, 2003.

[7] R. Prasher, "Surface Chemistry and characteristic based model for thermal contact resistance of fluidic interstitial thermal interface materials," Journal of Heat Transfer, vol. 123, pp. 969-975, 2001.

[8] J.P Gwinn and R. L. Webb, "Performance and testing of thermal interface materials," Microelectronics Journal, Volume 34, Issue 3, pp. 215-22, 2002.

[9] R. Prasher, "Rheology based modeling and desing of particle laden plymeric thermal interface material," Components and Packaging Technologiesm IEE Transactions, vol. 28, no. 2,pp. 230-237, 2005.

[10] P. Zhou. and K.. E. Goodson, "Modelling and measurement of pressure-dependent junction-spreader thermal resistance for integrated circuits,"ASME-Publications HTD, vol 369, pp.51-58, 2001.

[11] R. Prasher and J. Matayabus, "Thermal contact resitance of cured gel polymeric thermal interface material," Compnents and Packaging Technologies, IEEE Transactions, vol. 27, no. 4,pp. 702-709, 2004.

[12] R. Prasher, "Thermal boundary resistance of nanocomposites," International Journal of Heat and Mass Transfer, vol. 48,pp. 4942-4952, 2005.

[13] R. Prasher, "Acoustic mismatch model for thermal contact resistance of van der Waals contacts,"Applied Physics Letters, vol. 94, pp. 1905, 2009.

[14] S. Kaur, N. Raravikar, B.A. Helms, R, Prasher and D.F. Ogletree, "Enhaced thermal transport at covalently functionalized carbon nanotube array interfaces," Nature Communications, vol. 5, 2014.

[15] A. Devpura,P.E. Phelan, R. Prasher "Percolation theoryapplied to the analysis of thermal interface materials in flip-chip technology." Thermal and Thermomechanical Phenomena in Electronic Systems, 2000. ITHERM 2000. The Seventh Intersociety Conference on. Vol 1. IEEE, 2000.

[16] R.C. Progelhof, J. L. Throne and R.R. Ruetsch, "Methods for predicting the thermal conductivity of composite systems: a review" Polymer Engineering & Science vol.

16, no. 9,pp. 615-625, 1976.

[17] S. Shenogin, L. Xue, R. Ozisik, P. Keblinski, D.G. Cahill, "Role of thermal boundary resistance on the heat flow in carbon-nanotube composites", Journal of Applied Physics, vol. 95, no. 12, pp. 8136-8144, 2004.

[18] M.B. Bryning, D.E. Milkie, M.F. Islam, J.M. Kikkawa and A. G. Yodth,"Thermal conductivity and interfacial resistance in single-wall carbon nanotube epoxy composites,"Applied Physics letters, vol. 87,pp. 161909 2005.

[19] E.T. Swartz, R. O. Pohl, "Thermal Boundary Resistance", Reviews of moderm Physics, vol. 61, no. 605, 1989.

[20] P. Kapitza,"Heat Transfer and Superfluidity of Helium II", vol. 4, pp. 354, 1941.

[21] C.-W. Nan, R. Birringer, D. R. Clarke and H. Gleiter, "Effective Thermal Conductivity of Particulate Composites with Interfacial Thermal Resistance," *Journal of Appied Physics,* vol. 10, pp. 6692-6699, 1997.

[22] I.M. Khalatnikov and I.N. Adamenko. "Theory of the Kapitza temperature discontinuity at a solid body-liquid helium boundary." Soviet Journal of Experimental and Theoretical Physics, vol 36, pp. 391, 1973

[23] E. Swartz and R. Pohl,"Thermal resitance at interfaces", Applied Physics Letters, vol. 51, pp. 2200-2202, 1987.

[24] C.-W. Nan, "Physics of inhomogeneous inorganic materials," *Progress in materials science,* vol. 37, pp. 1-116, 1993.

[25] D. Hasselman and L. Johnson, "Heat Conduction characteristics of a carbon-fibre-reinforced lithia-alumino-silicate glass ceramic," *Journal of material Science,* vol. 22, pp. 701-709, 1987.

[26] H. Hatta and M. Taya, "Thermal conductivity of coated filler composites," *Journal of Applied Physics,* vol. 59, pp. 1851-1860, 1986.

[27] Y. Benveniste and T. Miloh, "The effective conductivity of composites with imprfect thermal contact at constituent interfaces," *International Journal of Engineering Science,* vol. 24, pp. 1537-1552, 1986.

[28] S. Iijima, "Helical microtubules of graphitic carbon. Nature Ization", Chem Phys Lett. , vol. 243, pp. 354, 1991.

[29] S. Ruoff, D. Rodney, D. Qian and W. Kam Lu, "Mechanical properties of carbon nanotubes: theoretical predictions and experimental measurements," Comptes Rendus Physique 4, vol 9, pp. 993-1008, 2003.

[30] C. Subramaniam, T. Yamada, K. Kobashi, A. Sekiguchi,D.N. Futaba, M. Yumura, and K. Hata "One hundred fold increase in current carrying capacity in a carbon nanotube-copper composite," Nature communications, vol. 4, 2013.

[31] C. Bins, "Carbon Nanostructures: Bucky Balls and Nanotubes,"*Introduction to Nanoscience and Nanotechnology*, 53-95, 2010.

[32] D. W. Park and S. E. Shim, "A review on thermal conductivity of polymer composites using carbon-based fillers: Carbon Nanotubes and Carbon Fibers.," Carbon letters, vol. 11, no. 4, pp. 347-356, 2010.

[33] L. Nielsen, "The thermal an electrical conductivity of two-phase systems," Industrial & Engineering chemistry fundamentals vol. 13, no. 1,pp. 17-20, 1974.

[34] F.H. Gojny, M. H. Wichmann, B. Fiedler, I.A. Kinloch, W. Bauhofer, A.H. Windle and K. Schulte, "Evaluation and identification of electrical and thermal conduction mechanisms in carbon nanotube/epoxy composites" Polymer, vol. 47, pp. 2036-2045, 2006.

[35] Kashiwagi, Takashi, Fangming Du, Karen I. Winey, Katrina M. Groth, J. R. Shields, Severine P. Bellayer, Hansoo Kim, and Jack F. Douglas. "Flammability properties of polymer nanocomposites with single-walled carbon nanotubes: effects of nanotube dispersion and concentration." *Polymer* 46, no. 2 ,pp. 471-481, 2005

[36] H. Xia and M. Song. "Preparation and characterization of polyurethane–carbon nanotube composites." *Soft Matter* 1, no. 5,pp. 386-394, 2005

[37] Xu, Yunsheng, Gunawidjaja Ray, and Beckry Abdel-Magid. "Thermal behavior of single-walled carbon nanotube polymer–matrix composites." *Composites Part A: Applied Science and Manufacturing* 37, no. 1, pp. 114-121, 2006

[38] S. Misra and J. Timmerman. "Thermally Conductive Liquid Materials for Electronics Packaging." In *IMAPS Advanced Technology Workshop on Thermal Management, Palo Alto, CA*. 2009.

[39] D. D. L. Chung"Materials for thermal conduction." *Applied thermal engineering* 21, no. 16, pp. 1593-1605, 2001

[40] J. Xu, and T. S. Fisher. "Thermal Contact Conductance Enhancement With Carbon Nanotube Arrays." In *ASME 2004 International Mechanical Engineering Congress and Exposition*, pp. 559-563. American Society of Mechanical Engineers, 2004.

[41] Choi, S. U. S., Z. G. Zhang, Wu Yu, F. E. Lockwood, and E. A. Grulke. "Anomalous thermal conductivity enhancement in nanotube suspensions." *Applied physics letters* 79, no. 14 (2001): 2252-2254.

[42] M.J Biercuk, Mark C. Llaguno, M. Radosavljevic, J. K. Hyun, Alan T. Johnson, and John E. Fischer. "Carbon nanotube composites for thermal management." *Applied physics letters* 80, no. 15, pp. 2767-2769, 2002

[43] Hu, Xuejiao, Linan Jiang, and Kenneth E. Goodson. "Thermal conductance enhancement of particle-filled thermal interface materials using carbon nanotube inclusions." In *Thermal and Thermomechanical Phenomena in Electronic Systems, 2004. ITHERM'04. The Ninth Intersociety Conference on*, pp. 63-69. IEEE, 2004.

[44] D. Fabris, M. Rosshirt, C.Cardenas, P. Wilhite, T. Yamada, and C. Y. Yang. "Application of carbon nanotubes to thermal interface materials." *Journal of Electronic Packaging* 133, no. 2 (2011): 020902.

[45] C-W Nan, G. Liu, Y. Lin, and M. Li. "Interface effect on thermal conductivity of carbon nanotube composites." *Applied Physics Letters* 85, no. 16 (2004): 3549-3551.

[46] C-W Nan. "Magnetoelectric effect in composites of piezoelectric and piezomagnetic phases." *Physical Review B* 50, no. 9 (1994): 6082.

[47] C-W Nan, Z. Shi, and Y. Lin. "A simple model for thermal conductivity of carbon nanotube-based composites." *Chemical Physics Letters* 375, no. 5 (2003): 666-669.

[48] J.R. Brockenbrough, S. Suresh, and H. A. Wienecke. "Deformation of metal-matrix composites with continuous fibers: geometrical effects of fiber distribution and

shape." *Acta metallurgica et materialia* 39, no. 5 (1991): 735-752.

[49] T. Christman, A. Needleman, and S. Suresh. "An experimental and numerical study of deformation in metal-ceramic composites." *Acta Metallurgica* 37, no. 11 (1989): 3029-3050..

[50] S. Ghosh, N. Zdzislaw, and L. Kyunghoon. "Quantitative characterization and modeling of composite microstructures by Voronoi cells." *Acta Materialia* 45, no. 6 (1997): 2215-2234.

[51] S. Ghosh, L. Kyunghoon, and S. Moorthy. "Multiple scale analysis of heterogeneous elastic structures using homogenization theory and Voronoi cell finite element method." *International Journal of Solids and Structures* 32, no. 1 (1995): 27-62.

[52] S. Ghosh, and M. Suresh. "Elastic-plastic analysis of arbitrary heterogeneous materials with the Voronoi cell finite element method." *Computer Methods in Applied Mechanics and Engineering* 121, no. 1 (1995): 373-409.

[53] S. Ghosh, and L. Yunshan. "Voronoi cell finite element model based on micropolar theory of thermoelasticity for heterogeneous materials." *International journal for numerical methods in engineering* 38, no. 8 (1995): 1361-1398.

[54] S. Moorthy and S. Ghosh. "A model for analysis of arbitrary composite and porous microstructures with Voronoi cell finite elements." *International journal for numerical methods in engineering* 39, no. 14 (1996): 2363-2398.

[55] D.Souvaine, M. Horn, and J. Weber, "Voronoi Diagrams: computational geometry course" Tufts University, 2005..

[56] W.A Spitzig, J.F. Kelly, and O. Richmond, "Quantitative characterization of second-phase populations," Metallography, vol. 18, pp 235-261 1985

[57] A. Bejan, Convection Heat Transfer, fourth edition, 2013 Jonh Wiley & Sons.

[58] Gharagozloo-Hubmann, Kati, A. Boden, G. JF Czempiel, I.Firkowska, and S.Reich. "Filler geometry and interface resistance of carbon nanofibres: Key parameters in thermally conductive polymer composites." *Applied Physics Letters* 102, no. 21 (2013): 213103.

[59] Devpura, Amit, P. E. Phelan, and R.S. Prasher. "Percolation theory applied to the analysis of thermal interface materials in flip-chip technology." In *Thermal and Thermomechanical Phenomena in Electronic Systems, 2000. ITHERM 2000. The Seventh Intersociety Conference on*, vol. 1. IEEE, 2000.

[60] S. Torquato , and M. D. Rintoul. "Effect of the interface on the properties of composite media." *Physical Review Letters* 75, no. 22 (1995): 4067.

[61] "Electronic Equipment Failures: Cause, Effect and Resolution," *IEN Indsutrial Equipment News*, 2013.

[62] R. University of California, "Methods for producing high efficiciency thermal materials with Graphene and metal fillers". Riverside/CA 2013.

[63] Hu, Xuejiao, L. Jiang, and K. E. Goodson. "Thermal conductance enhancement of particle-filled thermal interface materials using carbon nanotube inclusions." In *Thermal and Thermomechanical Phenomena in Electronic Systems, 2004. ITHERM'04. The Ninth Intersociety Conference on*, pp. 63-69. IEEE, 2004.

[64] Gharagozloo-Hubmann, Kati, A. Boden, G. JF Czempiel, I. Firkowska, and S.Reich.

"Filler geometry and interface resistance of carbon nanofibres: Key parameters in thermally conductive polymer composites." *Applied Physics Letters* 102, no. 21 (2013): 213103.